

Optimal network online change point localisation

Yi Yu¹, Oscar Hernan Madrid Padilla², Daren Wang³, and Alessandro Rinaldo⁴

¹Department of Statistics, University of Warwick

²Department of Statistics, University California, Los Angeles

³Department of Statistics, University of Notre Dame

⁴Department of Statistics & Data Science, Carnegie Mellon University

December 30, 2021

Abstract

We study the problem of online network change point detection. In this setting, a collection of independent Bernoulli networks is collected sequentially, and the underlying distributions change when a change point occurs. The goal is to detect the change point as quickly as possible, if it exists, subject to a constraint on the number or probability of false alarms. In this paper, on the detection delay, we establish a minimax lower bound and two upper bounds based on NP-hard algorithms and polynomial-time algorithms, i.e.

$$\text{detection delay} \begin{cases} \gtrsim \log(1/\alpha) \frac{\max\{r^2/n, 1\}}{\kappa_0^2 n \rho}, \\ \lesssim \log(\Delta/\alpha) \frac{\max\{r^2/n, \log(r)\}}{\kappa_0^2 n \rho}, & \text{with NP-hard algorithms,} \\ \lesssim \log(\Delta/\alpha) \frac{r}{\kappa_0^2 n \rho}, & \text{with polynomial-time algorithms,} \end{cases}$$

where κ_0, n, ρ, r and α are the normalised jump size, network size, entrywise sparsity, rank sparsity and the overall Type-I error upper bound. All the model parameters are allowed to vary as Δ , the location of the change point, diverges.

The polynomial-time algorithms are novel procedures that we propose in this paper, designed for quick detection under two different forms of Type-I error control. The first is based on controlling the overall probability of a false alarm when there are no change points, and the second is based on specifying a lower bound on the expected time of the first false alarm. Extensive experiments show that, under different scenarios and the aforementioned forms of Type-I error control, our proposed approaches outperform state-of-the-art methods.

Keywords: Dynamic networks, online change point detection, minimax optimality.

1 Introduction

In this paper we are concerned with online change point detection in dynamic networks. To be specific, we observe a sequence of independent adjacency matrices $\{A(t), t = 1, 2, \dots\}$, with $\mathbb{E}\{A(t)\} = \Theta(t)$, for $t \in \mathbb{N}_+$. If there exists $t^* \geq 2$, such that $\Theta(t^*) \neq \Theta(t^* - 1)$, then we call t^* a change point. Our aim is to detect the existence of such change points as soon as they occur. On

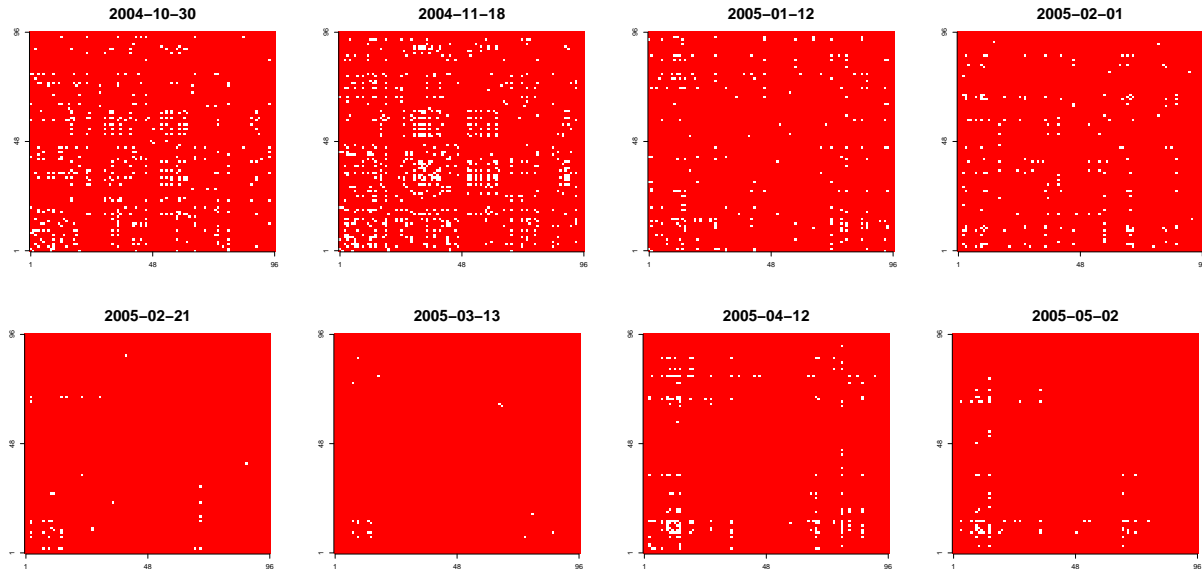


Figure 1: Interaction networks based on the MIT cellphone data sets. A white dot means the corresponding row and column individuals interacted on the specific date. A red dot means the lack of interaction. Details are explained in Section 4.3.

the other hand, if there is no change point, then we would like to avoid false alarms. To the best of our knowledge, this problem has not been theoretically studied in the existing statistical literature.

The problem we described above is an abstractification of various real-life problems. For instance, in cybersecurity, one monitors the internet or a system and wishes to detect malicious activity as early as it starts. In finance, regulatory authorities oversee the markets and aim to stop unlawful activities at an early stage. In epidemiology, public health sectors follow the spreading of a contagious disease in a community and target at knowing the spreading pattern changes as they happen.

As a concrete example, we consider the Massachusetts Institute of Technology (MIT) cellphone data set (Eagle and Pentland, 2006). The data set consists of human interactions measured by the cellphone activity of the participants. There were 96 participants that included students and faculty members at the MIT. The data were taken from 14-Sept-2004 to 5-May-2005.

We construct two experiments to evaluate our proposed methods and our competitors. In the first example, we use the data from 14-Sept-2004 to 15-Feb-2005, which cover the MIT winter recess starting on 22-Dec-2004 and ending on 3-Jan-2005. In our second example, we use the data from 1-Jan-2005 to 5-May-2005, which cover the spring recess starting on 26-Mar-2005 and ending on 3-Apr-2005. In Figure 1, we plot the interaction networks for a few representative dates. A white dot means the corresponding row and column individuals interacted on the specific date, while a red dot means the lack of interaction. For these two examples, our proposed method detects change points at 27-Dec-2004 and 31-Mar-2005, respectively. Our competitors' change point estimators are around 30-Jan-2005 and 6-Apr-2005, respectively. Our method is clearly the best at detecting the winter and spring recess periods. Numerical details are explained in Section 4.3.

Due to the aforementioned real-world applications, change point detection problems have been intensively studied in the literature, not necessarily in the dynamic networks context though. In terms of online change point detection, i.e., making sequential decisions about the existence of change points while collecting data, [Lorden \(1971\)](#), [Moustakides \(1986\)](#), [Ritov \(1990\)](#), [Lai \(1981\)](#), [Lai \(1998\)](#), [Lai \(2001\)](#), [Chu et al. \(1996\)](#), [Aue and Horváth \(2004\)](#), [Kirch \(2008\)](#), [Madrid Padilla et al. \(2019\)](#) and [Yu et al. \(2020\)](#) studied univariate sequences; [He et al. \(2018\)](#) focused on a sequence of random graphs; [Chen \(2019\)](#) and [Dette and Gösmann \(2019\)](#) allowed for more general scenarios, including nonparametric models; [Chen et al. \(2020\)](#) and [Keshavarz et al. \(2018\)](#) studied high-dimensional Gaussian vectors. In terms of offline change point detection, i.e., after collecting a sequence of data, one seeks change points retrospectively, a wide range of models have been studied. The closely related one is [Wang et al. \(2018\)](#), where a sequence of adjacency matrices were considered. More discussions with existing literature will be provided as we unfold our results.

1.1 List of contributions

The contributions of this paper are summarised below.

- To the best of our knowledge, it is the first time that online change point detection is formally analysed in a sequence of adjacency matrices, allowing all model parameters to vary as functions of Δ .
- We establish minimax lower bounds on the detection delay. To the best of our knowledge, in statistical networks literature, a lower bound involving the rank parameter has only been established in estimation problems (e.g. [Gao et al., 2015](#)), but not in the context of testing, not to mention change point detection. Our lower bound matches, up to a logarithmic factor, an upper bound derived based on an NP-hard algorithm.
- In addition, we propose a computationally-efficient network online change point detection method, which comes with two variants corresponding to two different Type-I error controlling strategies. Extensive numerical results are provided to evaluate the performance of our proposed methods against state-of-the-art competitors. We also discuss tuning parameter selection aspects of our approaches.

Throughout this paper, we will adopt the following notation. For any matrix $M \in \mathbb{R}^{m_1 \times m_2}$, let $\|M\|_F$ and $\|M\|_\infty = \max_{i=1}^{m_1} \max_{j=1}^{m_2} |M_{ij}|$ be the Frobenius norm and the entry-wise supremum norm of M , respectively. For any two matrices $A, B \in \mathbb{R}^{m_1 \times m_2}$, let $(A, B) = \text{tr}(A^\top B)$ be the Frobenius inner product of two matrices.

2 Methods

Since our data are a sequence of adjacency matrices, our first task is to formally define the networks at every time point.

Definition 1 (Inhomogeneous Bernoulli networks). *A network with node set $\{1, \dots, n\}$ is an inhomogeneous Bernoulli network if its adjacency matrix $A \in \mathbb{R}^{n \times n}$ satisfies*

$$A_{ij} = A_{ji} = \begin{cases} 1, & \text{nodes } i \text{ and } j \text{ are connected by an edge,} \\ 0, & \text{otherwise;} \end{cases}$$

and $\{A_{ij}, i < j\}$ are independent Bernoulli random variables with $\mathbb{E}(A_{ij}) = \Theta_{ij}$. We refer to the matrix Θ as the graphon matrix.

This general definition includes popular network models as special cases, but it is not restricted to any specific model. Note that we allow every random variable that corresponds to an integer pair (i, j) , $1 \leq i < j \leq n$, to have its own mean, i.e. $\mathbb{E}(A_{ij}) = \Theta_{ij}$.

Remark 1. *Despite the flexibility it enjoys, Definition 1 is also subjected to a number of restrictions. First, each random variable is assumed to be Bernoulli, which is a sub-Gaussian random variable. However, our framework can be extended to handle Poisson random variables. The algorithms we propose in the sequel follow naturally, and the theoretical results can be adjusted by using sub-Exponential concentration inequalities. Second, the adjacency matrices are assumed to be symmetric in Definition 1. All the results in this paper can be extended straightforwardly to asymmetric cases, corresponding to directed networks. Finally, the model does not allow for dependence between entries of the adjacency matrix.*

In order to detect the change points of $\{\Theta(t), t = 1, 2, \dots\}$, we adopt the network CUSUM statistic, which originated in the univariate CUSUM statistics from [Page \(1954\)](#) and was first formally stated in [Wang et al. \(2018\)](#).

Definition 2. *Given a sequence of matrices $\{A(t)\}_{t=1,2,\dots} \subset \mathbb{R}^{n \times n}$, we define the corresponding online CUSUM statistics as*

$$\hat{A}_{s,t} = \sqrt{\frac{t-s}{st}} \sum_{l=1}^s A(l) - \sqrt{\frac{s}{(t-s)t}} \sum_{l=s+1}^t A(l),$$

for all integer pairs (s, t) , $t \geq 2$ and $s \in [1, t)$.

With the notation introduced in Definition 2, we have for any integer pair (s, t) , $1 \leq s < t$,

$$\mathbb{E}(\hat{A}_{s,t}) = \hat{\Theta}_{s,t} = \sqrt{\frac{t-s}{st}} \sum_{l=1}^s \Theta(l) - \sqrt{\frac{s}{(t-s)t}} \sum_{l=s+1}^t \Theta(l).$$

Algorithm 2 is our main procedure, with a subroutine detailed in Algorithm 1 and a variant in Algorithm 3. Both Algorithms 2 and 3 are written in a way that they will not stop if no change point is detected. In practice, they can be terminated either by users or if there are no more new data.

To motivate our algorithms, we first investigate the statistics in Definition 2. These are linear combinations of all adjacency matrices up to time point $t \geq 2$. To be specific, for $1 \leq s < t$, the corresponding statistic is a difference between the sample means before and after time point s . In the univariate online change point detection problem (e.g. [Yu et al., 2020](#)), one scans through all possible integer pairs (s, t) , $1 \leq s < t$. In Algorithm 2, we propose a more efficient algorithm to avoid scanning through all $s \in [1, t)$.

For every time point $t \geq 2$, in Algorithm 2, we only consider $s \in \mathcal{S}(t)$ for candidates of change points, where $\mathcal{S}(t) = \{t - 2^j, j = 0, 1, \dots, \lfloor \log(t)/\log(2) \rfloor - 1\}$ is a set of geometric scale grid points. Once the criteria

$$\|\tilde{B}_{s,t}\|_F > C \log^{1/2}(t/\alpha) \quad \text{and} \quad (\hat{A}_{s,t}, \tilde{B}_{s,t} / \|\tilde{B}_{s,t}\|_F) > b_t \quad (1)$$

are met, we declare that there exists a change point at t .

The criteria in (1) are constructed based on two independent samples $\{A(t)\}$ and $\{B(t)\}$. In practice, one can achieve this by splitting data into odd and even indices subsamples. For each integer pair (s, t) , the quantity $\tilde{B}_{s,t}$ is a function of the CUSUM statistic $\hat{B}_{s,t}$, obtained by the subroutine Algorithm 1. In fact, $\tilde{B}_{s,t}$ is a universal singular value thresholding (USVT) estimator. The USVT algorithm was proposed in Chatterjee (2015), for the purpose of estimating low-rank high-dimensional sparse matrices.

The criteria (1) have two components. We first need to check that the USVT estimator $\|\tilde{B}_{s,t}\|_F$ is large enough. In theory, this is required to prompt near optimal detection delay. Intuitively speaking, change points would only occur, if $\|\tilde{B}_{s,t}\|_F$ is large. Provided that this criterion holds, we then check that the matrix inner product $(\hat{A}_{s,t}, \tilde{B}_{s,t}/\|\tilde{B}_{s,t}\|_F)$ is large enough. The data splitting is summoned due to the fact that for any Bernoulli random variable X , $X^2 = X$. Therefore, in order to detect the change in terms of the Frobenius norm, data splitting helps to estimate the squared means of Bernoulli random variables.

In view of the whole procedure, there is a sequence of tuning parameters. The tuning parameters

$$\{\tau_{j,s,u}, j = 1, 2, u = 2, 3, \dots, s \in \mathcal{S}(u)\}$$

are used in the subroutine Algorithm 1. As suggested in Xu (2018), the parameters $\tau_{1,\cdot}$ serve as cutoffs of the upper bound on sample fluctuations; and the parameters $\tau_{2,\cdot}$ are chosen to be the entry-wise maximum norms of the matrices of interest. The tuning parameter $\alpha \in (0, 1)$ is the tolerance of Type-I errors and acts as an upper bound on the probability of returning at least one false alarm. The thresholds $\{b_t\}$ are upper bounds on the inner products when there is no change point. More detailed discussions and guidance on tuning parameter selection are provided in Sections 3 and 4.

Algorithm 1 Universal Singular Value Thresholding. USVT(A, τ_1, τ_2)

INPUT: Symmetric matrix $A \in \mathbb{R}^{n \times n}$, $\tau_1, \tau_2 > 0$.

$(\lambda_i, v_i) \leftarrow$ the i th eigen-pair of A , with $|\lambda_1| \geq \dots \geq |\lambda_n|$;

$A' \leftarrow \sum_{i: |\lambda_i| \geq \tau_1} \lambda_i v_i v_i^\top$;

$A'' \leftarrow$ a matrix with (i, j) th entry $(A'')_{ij}$ satisfying

$$(A'')_{ij} = \begin{cases} (A')_{ij}, & |(A')_{ij}| \leq \tau_2, \\ \text{sign}((A')_{ij})\tau_2, & |(A')_{ij}| > \tau_2. \end{cases}$$

OUTPUT: A'' .

In addition, we also present a variant of Algorithm 2 in Algorithm 3. Note that the main difference between these two algorithms is that the tuning parameter $\alpha \in (0, 1)$ is replaced by $\gamma \in \mathbb{N}$ in Algorithm 3. Inputs are changed correspondingly. These two algorithms represent two popular ways of controlling Type-I errors. The tuning parameter γ is in fact a lower bound on the average run length. In other words, a choice of γ implies that, when there is no change point, the expected time of the first false alarm is at least γ .

There is no algorithmic differences between Algorithms 2 and 3. Their theoretical differences will be explained in Section 3, and the tuning parameter selection differences will be discussed in Section 4.

Algorithm 2 Network online change point detection

INPUT: $\{A(u), B(u)\}_{u=1,2,\dots} \subset \mathbb{R}^{n \times n}$, $\{b_u, \tau_{1,s,u}, \tau_{2,s,u}, u = 2, 3, \dots, s = 1, 2, \dots, u\} \subset \mathbb{R}, \alpha \in (0, 1)$.
 $t \leftarrow 1$;
FLAG $\leftarrow 0$;
while FLAG = 0 **do**
 $t \leftarrow t + 1$;
 $J \leftarrow \lfloor \log(t)/\log(2) \rfloor$;
 $j \leftarrow 0$;
 while $j < J$ and FLAG = 0 **do**
 $s_j \leftarrow t - 2^j$;
 $\tilde{B}_{s_j,t} \leftarrow \text{USVT}(\hat{B}_{s_j,t}, \tau_{1,s_j,t}, \tau_{2,s_j,t})$;
 FLAG = $\mathbb{1} \left\{ (\hat{A}_{t-s_j,t}, \tilde{B}_{t-s_j,t} / \|\tilde{B}_{t-s_j,t}\|_F) > b_t \right\} \mathbb{1} \left\{ \|\tilde{B}_{t-s_j,t}\|_F > C \log^{1/2}(t/\alpha) \right\}$;
 $j \leftarrow j + 1$;
 end while
end while
OUTPUT: t .

Algorithm 3 Network online change point detection – a variant

INPUT: $\{A(u), B(u)\}_{u=1,2,\dots} \subset \mathbb{R}^{n \times n}$, $\{b_u, \tau_{1,s,u}, \tau_{2,s,u}, u = 2, 3, \dots, s = 1, 2, \dots, u\} \subset \mathbb{R}, \gamma \in \mathbb{N}$.
 $t \leftarrow 1$;
FLAG $\leftarrow 0$;
while FLAG = 0 **do**
 $t \leftarrow t + 1$;
 $J \leftarrow \lfloor \log(t)/\log(2) \rfloor$;
 $j \leftarrow 0$;
 while $j < J$ and FLAG = 0 **do**
 $s_j \leftarrow t - 2^{j-1}$;
 $\tilde{B}_{s_j,t} \leftarrow \text{USVT}(\hat{B}_{s_j,t}, \tau_{1,s_j,t}, \tau_{2,s_j,t})$;
 FLAG = $\mathbb{1} \left\{ (\hat{A}_{s_j,t}, \tilde{B}_{s_j,t} / \|\tilde{B}_{s_j,t}\|_F) > b_t \right\} \mathbb{1} \left\{ \|\tilde{B}_{s_j,t}\|_F > C \log^{1/2}(\gamma) \right\}$;
 $j \leftarrow j + 1$;
 end while
end while
OUTPUT: t .

3 Theory

This section consists of all the theoretical results we develop in this paper, with all the technical details in the Appendix. This section is organised as follows. All the assumptions are stated and discussed in Section 3.1. The theoretical guarantees of Algorithms 2 and 3 are provided in Section 3.2. To investigate the fundamental limits, we established a minimax lower bound on the detection delay in Section 3.3, with an NP-hard procedure which is nearly minimax optimal studied in Section 3.4. To conclude, we provide some additional discussions through comparisons with existing work in Section 3.4.

3.1 Assumptions

Before arriving at our main results, we start by introducing some assumptions. The following three assumptions introduce the sparsity parameter, describe the one change point and no change point scenarios, respectively.

Assumption 1. Assume that $\{A(1), A(2), \dots\} \subset \mathbb{R}^{n \times n}$ is a sequence of inhomogeneous Bernoulli networks satisfying $\mathbb{E}\{A(i)\} = \Theta(i) \in \mathbb{R}^{n \times n}$, $i = 1, 2, \dots$, and

$$\sup_{i=1,2,\dots} \|\Theta(i)\|_{\infty} = \rho,$$

where $\rho n \geq \log(n)$.

Assumption 2 (One change point scenario). Assume that there exists $\Delta \in \mathbb{N}^*$ such that

$$\Theta(1) = \dots = \Theta(\Delta) = \Theta_1 \quad \text{and} \quad \Theta(\Delta + 1) = \Theta(\Delta + 2) = \dots = \Theta_2.$$

In addition, let

$$\kappa_0 = \frac{\kappa}{n\rho} = \frac{\|\Theta_1 - \Theta_2\|_F}{n\rho} > 0 \quad \text{and} \quad r = \text{rank}(\Theta_1 - \Theta_2).$$

Assumption 3 (No change point scenario). Assume that

$$\Theta(1) = \Theta(2) = \dots = \Theta.$$

In the one change point scenario, in view of Assumptions 1 and 2, we see that the change point detection problem is characterised by the following parameters: the network size n , the entry-wise sparsity parameter ρ , the size of the uncontaminated sample Δ , the normalised jump size κ_0 , and the low-rank parameter r .

The jump size κ is defined to be the Frobenius norm of the difference between two consecutive but distinct graphon matrices. The choice of the Frobenius norm is tailored to the context of dynamic networks. Arguably, the most popular statistical network model is the stochastic block models (Holland et al., 1983). If both Θ_1 and Θ_2 are graphon matrices of two stochastic block models, then the Frobenius norm can explicitly reflect the magnitude of the change, as compared to other matrix norms including the operator norm and the supremum norm. For instance, if the community structure stays unchanged, but the between community probability changes from p_1 to p_2 in a community of size $n/2$, then $\kappa = n|p_1 - p_2|/2$. If the between and within community probabilities, p_1 and p_2 , remain the same, but the community structure changes from a balanced 2-community network to a balanced 3-community network, then $\kappa = \sqrt{13/18}n|p_1 - p_2|$. Since $\kappa \in (0, n\rho]$, the normalised jump size κ_0 is scale free and satisfies that $\kappa_0 \in (0, 1]$.

Without further restrictions, the low-rank parameter r is allowed to be $r \in \{1, \dots, n\}$. Note that, the introduction of the parameter r is on the difference matrix and we allow for arbitrary structure of each graphon *per se*.

3.2 Main results

Recall that our missions are as follows. When there is a change point, we wish to declare the existence of the change point as soon as it appears. The distance between the change point estimator and the change point is called detection delay, which is to be minimised. On the other hand, it is also

vital to control the false alarms. When there is no change point, we either control the probability of declaring change points, or the expected time of the first false alarm. These two different ways of controlling false alarms are in fact Algorithms 2 and 3. Their theoretical guarantees are provided in Theorem 1 and Corollary 2, respectively. In the results presented in this section, we assume the existence of two independent sequences of adjacency matrices. In practice, this can be done by splitting the data sequence into odd and even index sequences.

Theorem 1. *For any $\alpha \in (0, 1)$, assume that the data $\{A(t), B(t)\}_{t=1,2,\dots}$ are two independent sequences of adjacency matrices satisfying Assumption 1. Let \hat{t} be the output of Algorithm 2 with inputs $\{A(t), B(t)\}_{t=1,2,\dots}$,*

$$b_u = C_1 \sqrt{\rho \log\left(\frac{u}{\alpha}\right)}, \quad \tau_{1,s,u} = C \sqrt{n\rho} + \sqrt{2 \log\left\{\frac{u(u+1) \log(u)}{\alpha \log(2)}\right\}} \quad \text{and} \quad \tau_{2,s,u} = \sqrt{\frac{(u-s)s}{u}} \rho.$$

(i) (No change point.) *If $\{A(t), B(t)\}_{t=1,2,\dots}$ in addition satisfy Assumption 3, then it holds that*

$$\mathbb{P}\left\{\bigcap_{m \in \mathbb{N}} \{\hat{t} > m\}\right\} > 1 - \alpha.$$

(ii) (One change point.) *If $\{A(t), B(t)\}_{t=1,2,\dots}$ in addition satisfy Assumption 2, and there exists a large enough absolute constant $C_{\text{SNR}} > 0$ such that*

$$\Delta \kappa_0^2 n \rho > C_{\text{SNR}} r \log(\Delta/\alpha), \quad (2)$$

then

$$\mathbb{P}\left\{0 < \hat{t} - \Delta < \frac{C_d r n \rho \log(\Delta/\alpha)}{\kappa^2} = \frac{C_d r \log(\Delta/\alpha)}{\kappa_0^2 n \rho}\right\} > 1 - \alpha,$$

where $C, C_1, C_d > 0$ are absolute constants.

We can see from Theorem 1(i) that when there is no change point, with probability at least $1 - \alpha$, Algorithm 2 will not raise any false alarm. On the other hand, if there is a change point, then it follows from Theorem 1(ii) that the detection delay is at most of order

$$\frac{r \log(\Delta/\alpha)}{\kappa_0^2 n \rho},$$

with probability at least $1 - \alpha$.

In fact, the condition (2) can be regarded as a sort of signal-to-noise ratio condition and is a mild constraint. We list a few special cases here.

- (Small sample size.) If $\kappa_0, \rho, r, \alpha \asymp 1$, then as long as $\Delta \gtrsim \log^2(\Delta)/n$, (2) holds. If the network size n is large, then this shows that Algorithm 2 can detect change points with a very small number of uncontaminated samples.
- (Large rank matrices.) If $\kappa_0 \asymp 1$, $\rho \asymp \log^2(n)/n$, $\alpha \asymp 1$ and $\Delta \asymp n$, then the rank parameter r is allowed to be $r \asymp n$. This means that provided the size of uncontaminated sample is comparable with the size of networks, then it is not necessary to have a low-rank assumption imposed on the difference of the graphons.

- (Small jump size.) If $\rho, r, \Delta, \alpha \asymp 1$, then, provided that $\kappa_0 \gtrsim n^{-1/2}$, condition (2) holds. This means that the normalised jump size can decrease to zero if the size of the network diverges.

Finally, we remark on the choices of the tuning parameters. As we have mentioned in Section 2, the tuning parameters $\{\tau_{1,s,u}\}$ are the cutoffs due to the low-rank parameter and $\{\tau_{2,s,u}\}$ are to bound the entry-wise maximum norms. The theoretical choices of these two sets of parameters can be found in Lemma 9, with the aim of ensuring the good performances of the USVT estimators. The tuning parameter α is completely determined by practitioners, reflecting the tolerance of Type-I errors. The sequence $\{b_u\}$ reflects an upper bound on the statistics' fluctuations when there is no change point. The rate of $\{b_u\}$ is determined in Lemma 8.

Corollary 2. *For $\gamma \geq 2$, assume that the data $\{A(t), B(t)\}_{t=1,2,\dots}$ are two independent sequences of adjacency matrices satisfying Assumption 1. Let \hat{t} be the output of Algorithm 3 with inputs $\{A(t), B(t)\}_{t=1,2,\dots}$,*

$$b_u = C_1 \sqrt{\rho \log(\gamma)}, \quad \tau_{1,s,u} = C \sqrt{n\rho} + \sqrt{2 \log \left\{ \frac{2(\gamma+1)\gamma \log(\gamma+1)}{\log(2)} \right\}} \quad \text{and} \quad \tau_{2,s,u} = \sqrt{\frac{(u-s)s}{u}} \rho.$$

(i) (No change point.) If $\{A(t), B(t)\}_{t=1,2,\dots}$ in addition satisfy Assumption 3, then

$$\mathbb{E}(\hat{t}) \geq \gamma,$$

where $\mathbb{E}(\hat{t})$, under Assumption 3, is called the average run length.

(ii) (One change point.) If $\{A(t), B(t)\}_{t=1,2,\dots}$ in addition satisfy Assumption 2, and it holds that

$$\gamma \geq \Delta \quad \text{and} \quad \Delta \kappa_0^2 n \rho > C_{\text{SNR}} r \log(\gamma), \quad (3)$$

where $C_{\text{SNR}} > 0$ is an absolute constant, then

$$\mathbb{P} \left\{ 0 < \hat{t} - \Delta < \frac{C_d r n \rho \log(\gamma)}{\kappa^2} = \frac{C_d r \log(\gamma)}{\kappa_0^2 n \rho} \right\} > 1 - \gamma^{-1}, \quad (4)$$

where $C, C_1, C_d > 0$ are absolute constants.

Corollary 2 is Theorem 1's counterpart based on Algorithm 3. Comparisons of Theorem 1(i) and Corollary 2(i) show that Algorithms 2 and 3 have different strategies in controlling the false alarms. Theorem 1(i) shows that the Type-I error across the whole time horizon is upper bounded by α if Algorithm 2 is deployed. In contrast, Corollary 2(i) ensures that if Algorithm 3 is used then the expected time of the first false alarm is at least γ .

Both of these two ways to control the false alarms are widely used in the literature. We show in Theorem 1 and Corollary 2 that, if $\gamma \geq \Delta$ and

$$\gamma \asymp \Delta/\alpha, \quad (5)$$

then these two methods provide the same order of detection delay. If $\gamma < \Delta$, then the same localisation rate of Corollary 2 holds for $\max\{\hat{t} - \Delta, 0\}$ instead of $\hat{t} - \Delta$.

Finally, we summarise the differences between Algorithms 2 and 3. Since both α and γ reflect the preferences on Type-I error control, these two tuning parameters can be specified by the users.

Although we have specified theoretical guidance on all the other tuning parameters, in practice, they still involve either unknown quantities or unspecified constants. In order to tune these parameters, Algorithm 3 might be handier. One may have access to historical data under the pre-change-point distribution, and tune all the tuning parameters such that the average run length is γ . This is less natural under the strategy of Algorithm 2, unless the whole time course has a pre-specified endpoint, since the Type-I error is across the whole time course. This is in fact how we tune the tuning parameters in Section 4 for Algorithm 2.

3.3 A lower bound

In Theorem 1, we show that we are able to detect change points with the order of the detection delay upper bounded by

$$\frac{r \log(\Delta/\alpha)}{\kappa_0^2 n \rho}. \quad (6)$$

In this subsection, we will investigate the optimality of this upper bound.

Proposition 3. *Assume that $\{A(t)\}_{t=1,2,\dots}$ is a sequence of independent adjacency matrices satisfying Assumptions 1 and 2. Denote the joint distribution of $\{A(t)\}_{t=1,2,\dots}$ as $P_{\kappa,\Delta}$. Consider the class of estimators \mathcal{D} defined as*

$$\mathcal{D} = \{T : T \text{ is a stopping time and satisfies } \mathbb{P}_\infty(T < \infty) \leq \alpha\},$$

where \mathbb{P}_∞ indicates $\Delta = \infty$. Then for sufficiently small $\alpha \in (0, 1)$, there exists an absolute constant $c > 0$ such that we have that

$$\inf_{\hat{t} \in \mathcal{D}} \sup_{P_{\kappa,\Delta}} \mathbb{E}_P \{(\hat{t} - \Delta)_+\} \geq \frac{c \log(1/\alpha)}{\kappa_0^2 n \rho} \max\{1, r^2/n\}.$$

The change point estimators are all stopping time random variables satisfying that the overall Type-I error is controlled by $\alpha \in (0, 1)$. The rate of the detection delay is lower bounded by

$$\frac{\log(1/\alpha)}{\kappa_0^2 n \rho} \max\{1, r^2/n\}.$$

This means in the low-rank regime $r \lesssim \sqrt{n}$, we have the lower bound $\log(1/\alpha) (\kappa_0^2 n \rho)^{-1}$; in the large-rank regime $r \gtrsim \sqrt{n}$, the lower bound is of the order $\log(1/\alpha) r^2 (\kappa_0^2 n^2 \rho)^{-1}$. In view of Proposition 3, we see that (6) is nearly-optimal, saving for a logarithmic factor, only in the extreme regimes, i.e. $r \asymp n$ or $r \asymp 1$.

It is then interesting to investigate the gap between the lower and upper bounds. Recall that in the graphon estimation problems, Gao et al. (2015) has shown that, the minimax rate of the mean squared error for estimating a rank- r graphon $\Theta \in \mathbb{R}^{n \times n}$ is

$$\inf_{\hat{\Theta}} \sup_{\Theta} \mathbb{E} \left\{ \frac{1}{n^2} \|\hat{\Theta} - \Theta\|_F^2 \right\} \asymp \frac{r^2 + n \log(r)}{n^2},$$

where the upper bound is achieved by an NP-hard algorithm. In fact, we can also adopt NP-hard procedures to match the lower bound in Proposition 3, up to logarithmic factors.

3.4 An NP-hard procedure on stochastic block models

In this subsection, we first focus on the stochastic block models (Holland et al., 1983).

Definition 3 (Sparse Stochastic Block Model). *A network is from a sparse stochastic block model with size n , sparsity parameter ρ , membership matrix $Z \in \mathbb{R}^{n \times r}$ and connectivity matrix $Q \in [0, 1]^{r \times r}$ if the corresponding adjacency matrix satisfies*

$$\mathbb{E}(A) = \rho Z Q Z^\top - \text{diag}(\rho Z Q Z^\top).$$

The membership matrix Z consists of n rows, each of which has one and only one entry being 1 and has all the entries being 0; moreover, Z is a column full rank matrix, i.e. $\text{rank}(Z) = r$. The sparsity parameter $\rho \in [0, 1]$ potentially depends on n .

As we have already pointed out, the stochastic block models are special cases of the inhomogeneous Bernoulli networks defined in Definition 1.

In Gao et al. (2015), an NP-hard estimator of stochastic block models' graphons is proposed. In this subsection, we will replace the USVT estimator defined in Algorithm 1 and used in Algorithm 2 by the NP-hard estimator studied in Gao et al. (2015). For completeness, we include the estimator construction below.

Definition 4 (An NP-hard graphon estimator). *For any positive integers n and r , $r \leq n$, let $\mathcal{Z}_{n,r} = \{z : \{1, \dots, n\} \rightarrow \{1, \dots, r\}\}$ be the collection of all possible mappings from $\{1, \dots, n\}$ to $\{1, \dots, r\}$. Given an adjacency matrix $A = (A_{ij}) \in \mathbb{R}^{n \times n}$, any $z \in \mathcal{Z}_{n,r}$ and any $Q = (Q_{ab}) \in \mathbb{R}^{r \times r}$, define the objective function*

$$L(Q, z) = \sum_{a, b \in \{1, \dots, r\}} \sum_{\substack{(i, j) \in z^{-1}(a) \times z^{-1}(b) \\ i \neq j}} (A_{ij} - Q_{ab})^2.$$

For any optimiser of the the objective function

$$(\hat{Q}, \hat{z}) \in \arg \min_{Q \in \mathbb{R}^{r \times r}, z \in \mathcal{Z}_{n,r}} L(Q, z),$$

the estimator is defined as $\check{\Theta} = (\check{\Theta}_{ij})_{i,j=1}^n \in \mathbb{R}^{n \times n}$, with

$$\check{\Theta}_{ij} = \check{\Theta}_{ji} = \hat{Q}_{\hat{z}_i \hat{z}_j}, \quad i > j$$

and $\check{\Theta}_{ii} = 0$. For notational simplicity, we write $\check{\Theta} = \text{NP}(A, r)$.

The new procedure for change point detection replaces the USVT subroutine in Algorithm 2 with the estimation detailed in Definition 4. We present the full algorithm below.

Corollary 4. *For any $\alpha > 0$, assume that the data $\{A(t), B(t)\}_{t=1,2,\dots}$ are two independent sequences of adjacency matrices satisfying Assumption 1. Let \hat{t} be the output of Algorithm 4 with inputs $\{A(t), B(t)\}_{t=1,2,\dots}$ and*

$$b_u = C_1 \sqrt{\rho \log \left(\frac{u}{\alpha} \right)}.$$

Algorithm 4 Network online change point detection - NP-hard

INPUT: $\{A(u), B(u)\}_{u=1,2,\dots} \subset \mathbb{R}^{n \times n}$, $\{b_u, u = 2, 3, \dots\} \subset \mathbb{R}$, $\alpha \in (0, 1)$, $r_0 \in \mathbb{N}^*$.

```
t ← 1;
FLAG ← 0;
while FLAG = 0 do
  t ← t + 1;
  J ← ⌊log(t)/log(2)⌋;
  j ← 0;
  while j < J and FLAG = 0 do
    s_j ← t - 2^j;
    B̃_{s_j,t} ← NP(A, r_0);
    FLAG = 1 { (Â_{t-s_j,t}, B̃_{t-s_j,t}/||B̃_{t-s_j,t}||_F) > b_t } 1 { ||B̃_{t-s_j,t}||_F > C log^{1/2}(t/α) };
    j ← j + 1;
  end while
end while
OUTPUT: t.
```

(i) (No change point.) If $\{A(t), B(t)\}_{t=1,2,\dots}$ in addition satisfy Assumption 3, then for any $m \in \mathbb{N}$,

$$\mathbb{P} \left\{ \bigcap_{m \in \mathbb{N}} \{\hat{t} > m\} \right\} > 1 - \alpha.$$

(ii) (One change point.) If $\{A(t), B(t)\}_{t=1,2,\dots}$ in addition satisfy Assumption 2, the input $r_0 \geq r$, and there exists a large enough absolute constant $C_{\text{SNR}} > 0$ such that

$$\Delta \kappa_0^2 n^2 \rho > C_{\text{SNR}} \{r^2 + n \log(r)\} \log(\Delta/\alpha),$$

then

$$\mathbb{P} \left\{ 0 < \hat{t} - \Delta < \frac{C_d \{r^2 + n \log(r)\} \rho \log(\Delta/\alpha)}{\kappa^2} = \frac{C_d \{r^2/n + \log(r)\} \log(\Delta/\alpha)}{\kappa_0^2 n \rho} \right\} > 1 - \alpha,$$

where $C, C_1, C_d > 0$ are absolute constants.

Corollary 4 provided us with an upper bound on the detection delay matching the lower bound in Proposition 3, saving for logarithmic factors. However, the detection delay in Corollary 4 is based on an NP-hard procedure in Algorithm 4, which has limited practical value.

Comparing the results in Theorem 1 and Corollary 4, we see that in the very extreme regimes, i.e. $r \asymp 1$ or $r \asymp n$, the detection delays obtained by the proposed polynomial-time and NP-hard algorithms achieve the same rates. Both estimators are nearly optimal, saving for logarithmic factors. Between the two extreme cases $r \asymp 1$ and $r \asymp n$, the NP-hard algorithm achieves sharper rates than the polynomial time algorithm. This phenomenon is inline with the computational and statistical tradeoffs observed in other high-dimensional statistical problems, e.g. Zhang et al. (2012), Loh and Wainwright (2013), to name but a few.

3.5 Comparisons with existing work

With all the theoretical results at hand, we are ready to provide some in-depth comparisons with existing work. Since we believe that our paper is the first ever providing theoretical results for network (in the sense of random matrices) online change point detection problems, the four papers we select in this subsection are all concerned with different but related problems.

Chen (2019) establishes a general framework for online change point detection. Provided a suitable notion of distance, a k -nearest-neighbour-based test statistic is used for testing the existence of the change points in a sequential manner. In Section 4, we consider three different statistics such that the methods from Chen (2019) can be used as our competitors. As for the theoretical results, Chen (2019) focused on the average run length. In our paper, we provide a range of results including detection delay, average run length and minimax lower bounds.

In statistics literature, the term “network” sometimes refers to the precision matrices in Gaussian graphical models, which are different from what we study in this paper. Keshavarz et al. (2018) and Keshavarz and Michailidis (2020) studied online change point detection in Gaussian graphical models. In addition to the model differences, both Keshavarz et al. (2018) and Keshavarz and Michailidis (2020) focused on the limiting distributions of the test statistics under the null and alternative distributions. We conjecture that a detection delay might be obtainable based on the results thereof, but the results are not explicit yet. On the other hand, in our paper, especially based on Theorem 1, it is straightforward that the overall probabilities of falsely detecting change points or missing change points are both upper bounded by α .

Wang et al. (2018) investigated an offline network change point detection problem, where a sequence of independent adjacency matrices are collected and change point estimators are sought retrospectively. Despite the difference, there are some interesting comparisons, which to some extent, reflect the connections between online and offline change point detection problems.

- (1) The detection delay in the online setting can be seen as the counterpart of the localisation error in the offline setting. The minimax lower bound on the localisation error in Wang et al. (2018) is of order $(\kappa_0^2 n^2 \rho)^{-1}$, while the minimax lower bound on the detection delay in this paper is of order $\log(1/\alpha)(\kappa_0^2 n \rho)^{-1}(r^2/n + 1)$. The extra $\log(1/\alpha)$ term is rooted in the fact that we need to control the Type-I error in online settings. The other differences are more interesting – obviously, the offline rate is better than the online rate. This is because, the *de facto* smallest sample size for a certain distribution in the offline scenario is Δ , while in the online scenario it is $\min\{\Delta, \text{detection delay}\}$.
- (2) In both online and offline settings, we have seen a computational and statistical tradeoff. Comparing Theorem 1 and Corollary 4, we see that NP-hard estimators can detect change points under a weaker condition and provide a smaller detection delay. In the offline setting, as Wang et al. (2018) has conjectured, by replacing the USVT estimator with the NP-hard estimator in Definition 4, one can achieve a nearly optimal localisation error under a weaker condition, than the one needed by the USVT estimator.

4 Numerical experiments

4.1 Simulation studies

Recall that in Section 2, we proposed a network online change point detection method in Algorithm 2, with a subroutine in Algorithm 1 and a variant in Algorithm 3. In this section, we will investigate the numerical performances of our proposed methods. Since there is no direct competitor available, we will tailor the k -nearest neighbours type method proposed in Chen (2019).

In order to make a fair comparison with Chen (2019) we consider its three different statistics, including: the “original” (ORI) which specifies the original edge-count scan statistic, the weighted edge-count scan statistic (W) and the generalised edge-count scan statistic (G). The statistics are computed with internal functions in the R (R Core Team, 2020) package gStream (Chen and Chu, 2019).

We consider two different forms of calibration. The first is based on the probability of raising a false alarm. Using 200 Monte Carlo simulations and values of $\alpha \in \{0.01, 0.05\}$, we choose the detection thresholds such that, the probability of raising a false alarm in the interval $[1, T_{\text{train}}]$ is α . The values of T_{train} are taken from the set $\{150, 200\}$. The second one is based on the average run length γ . We consider values of γ in the set $\{150, 200\}$ and calibrate the thresholds of the competing methods, based on 200 Monte Carlo simulations, to have average run length approximately γ under the pre-change model. For the data splitting required by Algorithms 2 and 3, in all of our experiments, the sequence of adjacency matrices $\{A(u)\}$ consists of the odd indices of the original sequence, and the sequence $\{B(u)\}$ of the even ones.

To evaluate the performance of different methods, we proceed as follows. For each generative model described below, we run $N = 100$ Monte Carlo simulations, where in each trial the data are collected in the interval $[1, T]$, $T = 300$. The change point Δ occurs at the time point 150. Each method provides an estimator \hat{t} , which can be ∞ if no change points are detected in $[1, T]$. We define $\tilde{t} = \min\{T, \hat{t}\}$ and compute the average detection delay

$$\text{Delay} = \frac{\sum_{j=1}^N 1_{\{\tilde{t} \geq \Delta\}} (\tilde{t} - \Delta)}{\sum_{j=1}^N 1_{\{\tilde{t} \geq \Delta\}}}.$$

We also report the proportion of false alarms

$$\text{PFA} = \frac{\sum_{j=1}^N 1_{\{\tilde{t} < \Delta\}}}{N}.$$

As for Algorithm 2, guided by Theorem 1, we set

$$\tau_{1,s,u} = 0.2\sqrt{n\hat{\rho}} + \frac{1}{15}\sqrt{2\log\left(\frac{2(u-s)(u-s+1)}{\alpha}\right)} \quad \text{and} \quad \tau_{2,s,u} = \sqrt{\frac{(u-s)s}{u}}\hat{\rho},$$

where $\hat{\rho}$ is an estimator of ρ , calculated as the 0.95-quantile of the quantities

$$\hat{p}_{i,j} = \sum_{t=1}^T A_{ij}(t), \quad i, j \in \{1, \dots, n\}, \quad i < j, \quad (7)$$

where the matrices $\{A(t)\}_t^T$ are part of the training data. In addition, we set

$$b_u = C_1 \sqrt{\hat{\rho} \log\left(\frac{u}{\alpha}\right)},$$

with C_1 tuned to give the desired false alarm rate.

With respect to Algorithm 3, guided by Corollary 2, we let

$$\tau_{1,s,u} = 0.2\sqrt{n\hat{\rho}} + \frac{\sqrt{2\log(2\gamma+2)}}{15} \quad \text{and} \quad \tau_{2,s,u} = \sqrt{\frac{(u-s)s}{u}}\hat{\rho},$$

where $\hat{\rho}$ is the 0.95-quantile of the quantities in (7). In addition, we let

$$b_u = C_1\sqrt{\hat{\rho}\log(\gamma)},$$

with the constant C_1 calibrated to such that before the change point the expect time of the first false alarm is γ .

We consider four different settings.

Scenario 1. This consists of a stochastic block model with 3 communities of sizes $\lfloor n/3 \rfloor$, $\lfloor n/3 \rfloor$ and $n - 2\lfloor n/3 \rfloor$. The network size n takes values in $\{100, 150\}$. Denoting by z_i the label of the community associated with node $i \in \{1, \dots, n\}$, the data are generated as

$$A_{ij}(t) \stackrel{\text{ind.}}{\sim} \text{Bernoulli}(\rho B_{z_i z_j}(t)),$$

where $\rho = 0.02$ and the matrices $B(t)$ satisfy

$$B(t) = \begin{pmatrix} 0.6 & 1.0 & 0.6 \\ 1.0 & 0.6 & 0.5 \\ 0.6 & 0.5 & 0.6 \end{pmatrix}, \quad t \in \{1, \dots, \Delta\}$$

and

$$B(t) = \begin{pmatrix} 0.6 & 0.5 & 0.6 \\ 0.5 & 0.6 & 1.0 \\ 0.6 & 1.0 & 0.6 \end{pmatrix}, \quad t \in \{\Delta + 1, \Delta + 2, \dots, T\}.$$

Scenario 2. This is also a stochastic block model. We now take the number of communities to be 5 and the number nodes in each community to be $n/5$ where $n \in \{100, 150\}$. Again we set $\rho = 0.02$ but let

$$B(t) = \begin{pmatrix} 0.9 & 0.2 & 0.2 & 0.2 & 0.2 \\ 0.2 & 0.9 & 0.2 & 0.2 & 0.2 \\ 0.2 & 0.2 & 0.9 & 0.2 & 0.2 \\ 0.2 & 0.2 & 0.2 & 0.9 & 0.2 \\ 0.2 & 0.2 & 0.2 & 0.2 & 0.9 \end{pmatrix}, \quad t \in \{1, \dots, \Delta\}$$

and

$$B(t) = \begin{pmatrix} 0.5 & 0.1 & 0.1 & 0.1 & 0.1 \\ 0.1 & 0.5 & 0.1 & 0.1 & 0.1 \\ 0.1 & 0.1 & 0.5 & 0.1 & 0.1 \\ 0.1 & 0.1 & 0.1 & 0.5 & 0.1 \\ 0.1 & 0.1 & 0.1 & 0.1 & 0.5 \end{pmatrix}, \quad t \in \{\Delta + 1, \Delta + 2, \dots, T\}.$$

Scenario 3. We consider a degree corrected block model (Karrer and Newman, 2011) with 3 communities of sizes $\lfloor n/3 \rfloor$, $\lfloor n/3 \rfloor$ and $n - 2\lfloor n/3 \rfloor$, where $n \in \{100, 150\}$. Let z_i be the community to which node i belongs, and define $v_i = \sqrt{i/n}$. The data are then generated as

$$A_{ij}(t) \sim \text{Bernoulli}(v_i v_j B_{z_i z_j}(t)),$$

where

$$B(t) = \begin{pmatrix} 0.9 & 0.1 & 0.1 \\ 0.1 & 0.9 & 0.1 \\ 0.1 & 0.1 & 0.9 \end{pmatrix}, \quad t \in \{1, \dots, \Delta\}$$

and

$$B(t) = \begin{pmatrix} 0.95 & 0.15 & 0.15 \\ 0.15 & 0.95 & 0.15 \\ 0.15 & 0.15 & 0.95 \end{pmatrix}, \quad t \in \{\Delta + 1, \Delta + 2, \dots, T\}.$$

Scenario 4. This is a random dot product graph (Young and Scheinerman, 2007) with fixed latent positions. First, we generate the latent positions $X \in \mathbb{R}^{n \times 5}$ as

$$X_{ij} \stackrel{\text{i.i.d.}}{\sim} \text{Unif}[0, 1], \quad i = 1, \dots, n, j = 1, \dots, 5,$$

which are kept fixed throughout our simulations. We then construct $\tilde{X} \in \mathbb{R}^{n \times 5}$ as

$$\tilde{X}_{ij} \stackrel{\text{i.i.d.}}{\sim} \text{Unif}[0, 1], \quad i = 1, \dots, n, j = 1, \dots, 5,$$

which are also kept fixed throughout our simulations. Finally, the data are generated as

$$A_{ij}(t) \sim \text{Bernoulli}\left(\frac{X_i^\top X_j}{\|X_i\| \|X_j\|}\right), \quad t \in \{1, \dots, \Delta\}$$

and

$$A_{ij}(t) \sim \text{Bernoulli}\left(\frac{Y_i^\top Y_j}{\|Y_i\| \|Y_j\|}\right), \quad t \in \{\Delta + 1, \Delta + 2, \dots, T\},$$

where $X_i, \tilde{X}_i \in \mathbb{R}^5$ are the i th rows of the matrices X and \tilde{X} , $\|\cdot\|$ is the ℓ_2 -norm of vectors, and

$$Y_i = \begin{cases} \tilde{X}_i, & i \leq \lfloor n/4 \rfloor, \\ X_i, & \text{otherwise.} \end{cases}$$

We collect the results in Figure 2, Tables 1 and 2. In Figure 2, we exhibit one realisation each for each scenario. Each row corresponds to each scenario, from the first to the fourth. In each row, the left two panels are realisations before change points, and the right two panels are the post change points realisations. It can be seen from Figure 2 that, these four scenarios cover different types of networks, and the change points are hard to spot with the naked eye.

Tables 1 and 2 correspond to the two different ways to control Type-I errors. We reiterate that Algorithm 2, Theorem 1 and Table 1 correspond to the strategy of controlling the overall Type-I error α . Algorithm 3, Corollary 2 and Table 2 correspond to the strategy of lower bounding the average run length γ .

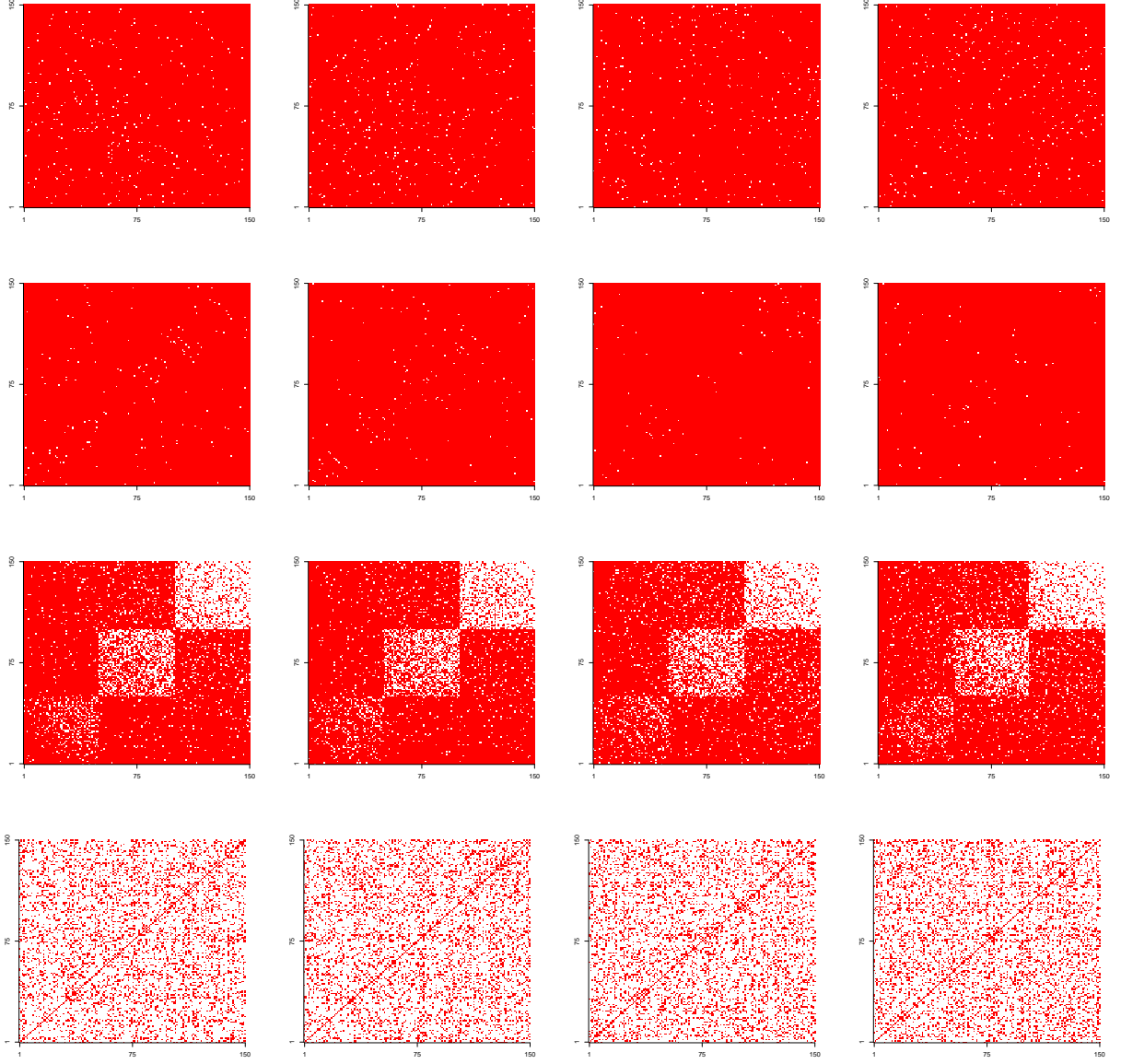


Figure 2: Examples of adjacency matrices generated under different scenarios. The first to the fourth rows correspond to the first to the fourth scenarios, respectively. In each row, from left to right, the first two plots correspond to networks generated before the change point, and the last two plots to networks generated after the change point. In each display, a white dot indicates one and a red dot indicates zero.

Table 1: Upper bounding overall Type-I errors: n , the network size; α , the Type-I error upper bound; T_{train} , the time length of the training data used for selecting tuning parameters; ORI, [Chen \(2019\)](#) using the original edge-count scan statistic; W, [Chen \(2019\)](#) using the weighted edge-count scan statistic; G, [Chen \(2019\)](#) using the generalised edge-count scan statistic.

Settings				Delay				PFA			
n	Scenario	α	T_{train}	Algo. 2	ORI	W	G	Algo. 2	ORI	W	G
150	1	0.01	200	35.38	145.92	147.44	147.44	0.00	0.02	0.00	0.00
150	1	0.05	200	32.93	135.41	137.42	137.42	0.02	0.04	0.03	0.03
150	1	0.01	150	33.10	145.92	146.08	146.08	0.02	0.02	0.00	0.00
150	1	0.05	150	30.61	140.09	139.55	139.55	0.02	0.03	0.02	0.02
100	1	0.01	200	89.74	147.66	148.97	148.97	0.00	0.02	0.00	0.00
100	1	0.05	200	54.90	135.94	142.88	142.88	0.05	0.07	0.05	0.05
100	1	0.01	150	73.14	148.95	149.83	149.83	0.00	0.02	0.00	0.00
100	1	0.05	150	50.52	135.94	141.77	141.77	0.06	0.04	0.05	0.05
150	2	0.01	200	25.00	149.36	150.00	150.00	0.00	0.00	0.00	0.00
150	2	0.05	200	22.84	149.14	146.16	146.16	0.05	0.05	0.03	0.03
150	2	0.01	150	24.64	150.00	148.39	148.39	0.00	0.00	0.02	0.02
150	2	0.05	150	22.34	149.14	144.76	144.76	0.02	0.06	0.05	0.05
100	2	0.01	200	92.90	150.00	150.00	150.00	0.05	0.01	0.02	0.02
100	2	0.05	200	68.48	150.00	147.35	145.88	0.06	0.03	0.04	0.04
100	2	0.01	150	92.94	150.00	150.00	150.00	0.02	0.02	0.01	0.01
100	2	0.05	150	68.48	149.12	150.00	150.00	0.06	0.04	0.03	0.03
150	3	0.01	200	26.62	150.00	148.61	73.05	0.00	0.02	0.03	0.03
150	3	0.05	200	17.74	147.23	140.67	62.88	0.02	0.06	0.04	0.04
150	3	0.01	150	25.54	150.00	150.00	76.54	0.00	0.01	0.01	0.02
150	3	0.05	150	17.11	146.80	138.90	59.85	0.03	0.05	0.04	0.04
100	3	0.01	200	38.36	150.00	149.85	75.98	0.01	0.00	0.01	0.01
100	3	0.05	200	35.48	149.19	148.45	64.6	0.02	0.02	0.05	0.05
100	3	0.01	150	35.23	149.57	149.85	77.01	0.01	0.00	0.01	0.01
100	3	0.05	150	36.06	149.14	148.35	58.07	0.04	0.03	0.06	0.08
150	4	0.01	200	3.68	13.67	10.33	10.78	0.00	0.03	0.04	0.03
150	4	0.05	200	3.35	12.77	9.81	10.10	0.05	0.07	0.05	0.06
150	4	0.01	150	3.70	14.19	11.19	12.01	0.01	0.01	0.02	0.01
150	4	0.05	150	3.33	12.60	9.68	10.01	0.03	0.07	0.05	0.04
100	4	0.01	200	4.00	16.51	13.12	13.12	0.00	0.00	0.00	0.00
100	4	0.05	200	3.80	14.28	12.05	12.03	0.04	0.05	0.03	0.05
100	4	0.01	150	4.00	16.95	12.66	12.62	0.00	0.00	0.02	0.03
100	4	0.05	150	4.00	14.91	12.14	12.12	0.05	0.03	0.03	0.05

We can see that if we choose to upper bound the overall Type-I error, then Algorithm 2 outperforms all three versions of [Chen \(2019\)](#). If we choose to lower bound the average run length, then Algorithm 3 still outperforms all three competitors except in all instances of Scenario 2. In fact, Algorithm 2 also performs worst in Scenario 2 out of all four scenarios. A possible reason why most methods suffer with Scenario 2 is that this is the model that has the largest r , the rank of

Table 2: Lower bounding the average run lengths: n , the network size; γ , the average run length lower bound; ORI, [Chen \(2019\)](#) using the original edge-count scan statistic; W, [Chen \(2019\)](#) using the weighted edge-count scan statistic; G, [Chen \(2019\)](#) using the generalised edge-count scan statistic.

Settings			Delay				PFA			
n	Scenario	γ	Algo. 3	ORI	W	G	Algo. 3	ORI	W	G
150	1	150	20.77	71.09	80.92	70.26	0.28	0.56	0.50	0.54
150	1	200	23.56	93.52	101.94	103.66	0.18	0.32	0.32	0.34
100	1	150	29.57	88.01	75.59	101.90	0.34	0.52	0.56	0.56
100	1	200	34.71	97.54	104.00	105.75	0.22	0.31	0.28	0.28
150	2	150	22.08	136.65	10.00	2.22	0.11	0.48	0.62	0.64
150	2	200	23.48	139.94	17.3	12.76	0.06	0.30	0.41	0.41
100	2	150	44.58	121.55	58.78	64.15	0.52	0.60	0.62	0.62
100	2	200	51.83	133.44	59.92	56.46	0.52	0.46	0.46	0.49
150	3	150	9.44	119.12	102.64	33.78	0.00	0.50	0.66	0.62
150	3	200	11.08	128.34	112.76	37.82	0.00	0.32	0.40	0.42
100	3	150	22.17	115.76	114.00	38.66	0.08	0.66	0.52	0.46
100	3	200	24.97	141.5	133.59	42.20	0.06	0.44	0.37	0.32
150	3	150	2.21	9.00	7.53	7.82	0.45	0.53	0.48	0.54
150	3	200	2.37	10.21	8.48	8.81	0.26	0.36	0.38	0.37
100	3	150	3.80	10.28	9.59	9.59	0.18	0.50	0.47	0.58
100	3	200	3.95	10.97	9.88	10.63	0.13	0.30	0.30	0.28

the difference of the graphons. It is understood that the USVT algorithm (Algorithm 1 [Chatterjee, 2015](#)) is less effective when the rank is relatively large. This is also reflected in the detection delay rate, which is linear in r .

4.2 Stock market data

We consider stock market data from April 1990 to January 2012. The data consist of the weekly log returns for the Dow Jones Industrial Average index and they are available in the R ([R Core Team, 2020](#)) package `ecp` ([James et al., 2019](#)). To construct networks, we first use a sliding window of window width being 3, and consider the covariance matrix among 29 companies' log-weekly-returns over a 3 week period. We then truncate the covariance matrices by setting those entries which have values above the 0.95-quantile as 1, and the remaining as 0. This construction leads to sparse networks. Some examples of these networks are illustrated in the first two rows of Figure 3.

As competitors to our estimator, we consider the same statistics (ORI), (W) and (G) from [Chen \(2019\)](#) that were used in Section 4.1. To evaluate the performances of these methods, we have chosen two periods of the original data, each consisting of a training set and a test set. We calculate the maximum score of each method using the training data and use the maximum score as the threshold for detecting false alarms.

In the first period, the data from 2-Apr-1990 to 4-Jan-1999 are used as the training set, and the data from 25-Jan-1999 to 31-May-2004 are used as the test set. The algorithm we proposed in Algorithm 2 detects a change point corresponding to 25-Mar-2002. This seems to coincide with

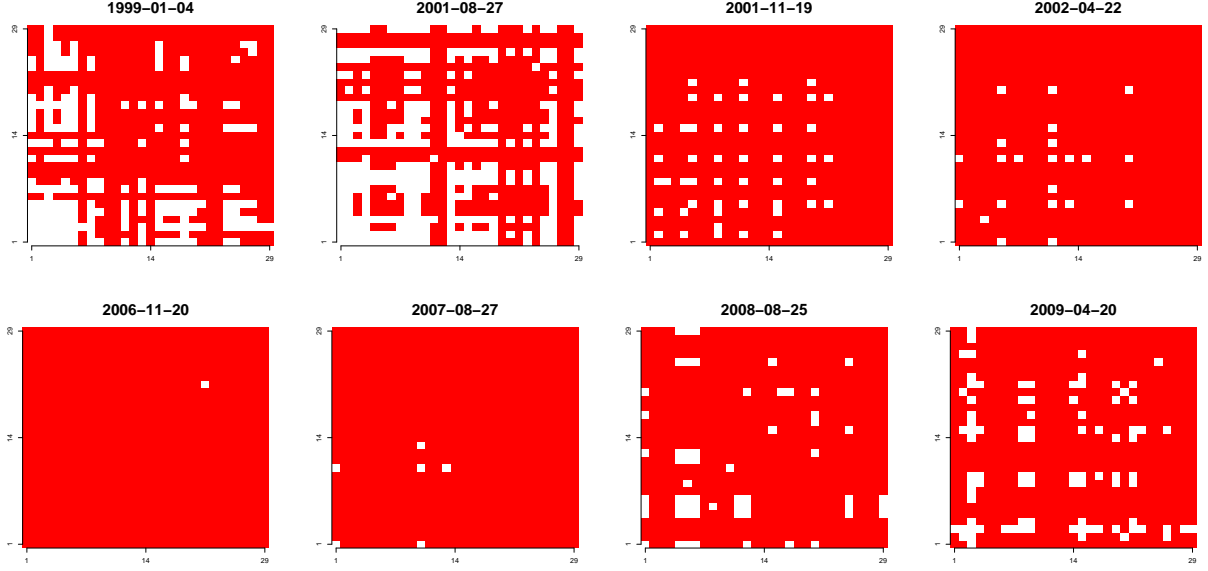


Figure 3: Stock market data set described in Section 4.2.

the period of financial turbulence after the 11-Sep-2001 terrorist attacks. We can also see in the first row of Figure 3 that there seems to be a change in pattern around such date. In contrast, the competitor methods did not detect the change point with the given choice of threshold.

In the second period, the data from 31-May-2004 to 15-Jan-2007 are used as the training set, and the data from 5-Feb-2007 to 1-Mar-2010 are used as the test set. We remark that the training data correspond to the period before the financial crisis of 2007–2008. Algorithm 2 detects a change point corresponding to the date 10-Mar-2008. The competing approaches detect a change point in the same period. Specifically, ORI detects the date December 17, 2007; and both W and G detect the date 19-Mar-2007. From looking at the second row of Figure 3, we can see that the 2007-2008 financial crisis seems to affect the network patterns in the data.

4.3 MIT cellphone data

In Section 1, we have studied the MIT cellphone data set. In this subsection, we provide all numerical details.

Originally, the data are in the form of 1392 networks of size 96×96 . For each day of the experiment, the data include four networks corresponding to six hours interval in the given day. We sum the four networks during each day resulting in 232 networks, each with 96 nodes. The networks are transformed to binary networks by setting all strictly positive entries as 1. In other words, in each binary network, if the entry (i, j) equals 1, then it means that participants i and j were within physically close proximity during the corresponding day.

To evaluate the performances of different methods, we construct two experiments. In the first we use the data from 14-Sept-2004 to 1-Dec-2004 as the training data set, and the data from 2-Dec-2004 to 15-Feb-2005 as the test set. The training set is the period before the MIT winter recess, which that year took place from 22-Dec-2004 to 3-Jan-2005. The thresholds are chosen in the same

way as Section 4.2. Algorithm 2 detects a change point on 27-Dec-2004; ORI on 30-Jan-2005; W and G on 29-Jan-2005. Clearly, our method is the best at detecting the winter recess period.

In our second example, we use the data from 1-Jan-2005 to 3-Mar-2005 as the training data set and the data from 4-Mar-2005 to 5-May-2005 as the test set. Thus the training data consist of networks before the spring recess which took place from 26-Mar-2005 to 3-Apr-2005. Algorithm 2 detects a change point on 31-Mar-2005; and ORI on 6-Apr-2005. Thus, our method seems to be quicker at detecting the spring recess.

5 Discussions

In this paper, we are concerned with online change point detection in a sequence of inhomogeneous Bernoulli networks. We established the minimax lower bound on the detection delay, which matches an upper bound, saving for logarithmic factors, based on an NP-hard estimation procedure. In addition, we proposed a polynomial-time algorithm, the detection delay of which matches the that based on NP-hard estimators in the extreme cases, i.e. $r \asymp 1$ and $r \asymp n$.

Our proposed methods consist of two different Type-I error control strategies, with the worst case computational cost of order $O(\log(t)\text{Cost}(n))$ when proceeding to the time point t , where $\text{Cost}(n)$ is the computational cost for running the USVT algorithm (Algorithm 1) on a size- n network.

In this paper, we only discuss the at most one change point scenario. In fact, it is straightforward to extend the algorithm and the results to multiple change points scenario. To be specific, one can restart the algorithm whenever a change point is declared by Algorithm 2. As for the theoretical results, in Theorem 1, we can let Δ be the minimal spacing between two consecutive change points. Provided that

$$C_{\text{SNR}}nr \log(\Delta/\alpha) > 2C_d,$$

then with probability at least $1 - \alpha$, all change points can be detected with detection delay uniformly upper bounded by the same detection delay upper bound in Theorem 1 and without false alarms. This is a straightforward consequence of Theorem 1, therefore we omit the technical details here.

In the existing literature, it is hoped to have an online change point detection with constant cost proceeding to every time point. In this sense, our cost $O(\log(t))$ is not efficient enough. However, to the best of our knowledge, when the before and after distributions are not fully specified, this constant computational cost is not achievable even in the univariate case. Having said this, it is still of vital interest to improve the computational efficiency of network online change point detection methods. We will leave this for future work.

Appendices

All necessary lemmas are collected in Appendix A and all proofs of the main results are left in Appendix B.

A Network change point lemmas

This lemma below is identical to Lemma S.6 in Wang et al. (2018), therefore we skip the proof here.

Lemma 5. (1) For any $t \in \mathbb{N}^*$, let $\{A(l)\}_{l=1}^t$ be a collection of independent matrices with independent Bernoulli entries satisfying

$$\max_{l=1, \dots, t} \|\mathbb{E}(A(l))\|_\infty \leq \rho,$$

with $n\rho \geq \log(n)$. Let $\{w_l\}_{l=1}^t \subset \mathbb{R}$ be a collection of scalars such that $\sum_{l=1}^t w_l^2 = 1$ and $\sum_{l=1}^t w_l = 0$. Then there exists an absolute constant $C > 32 \times 2^{1/4} e^2$ such that for any $\varepsilon > 0$,

$$\mathbb{P} \left(\left\| \sum_{l=1}^t w_l A(l) - \mathbb{E} \left(\sum_{l=1}^t w_l A(l) \right) \right\|_{\text{op}} \geq C\sqrt{n\rho} + \varepsilon \right) \leq \exp(-\varepsilon^2/2). \quad (8)$$

(2) If $\{A(l)\}_{l=1}^t$ are symmetric matrices, then (8) still holds.

Lemmas 6 and 7 are from Lemma 1 in Xu (2017).

Lemma 6. Let $A, B \in \mathbb{R}^{n \times n}$ be two symmetric matrices with $\|A - B\|_{\text{op}} < \tau/(1 + \delta)$, $\tau > 0$. Then for a fixed $\delta < 1$, we have

$$\|\text{USVT}(A, \tau, \infty) - B\|_{\text{F}}^2 \leq 16 \min_{s=0}^n \left\{ s\tau^2 + (1 + \delta)^2 \delta^{-2} \sum_{i=s+1}^n \lambda_i^2(B) \right\},$$

where $\lambda_n(B) \geq \dots \geq \lambda_1(B)$ are the eigenvalues of B .

Lemma 7. Let A and B be defined as in Lemma 6, and that $\|B\|_\infty \leq \tau'$, then

$$\|\text{USVT}(A, \tau, \tau') - B\|_{\text{F}}^2 \leq 16 \min_{s=0}^n \left\{ s\tau^2 + (1 + \delta)^2 \delta^{-2} \sum_{i=s+1}^n \lambda_i^2(B) \right\},$$

where $\lambda_n(B) \geq \dots \geq \lambda_1(B)$ are the eigenvalues of B .

This lemma below is Lemma S.2 in Wang et al. (2018).

Lemma 8. Let $\{X(l)\}_{l=1,2,\dots} \in \mathbb{R}^p$ be a sequence of independent random vectors with independent Bernoulli entries. Suppose that $\mathbb{E}(X_i(t)) = \mu_i(t)$ and that

$$\sup_{l=1,2,\dots} \|\mu(l)\|_\infty \leq \rho.$$

For any $t > 1$, let $v \in \mathbb{R}^p$ and $\{w_l\}_{l=1}^t \subset \mathbb{R}$ satisfy $\sum_{l=1}^t w_l^2 = 1$. Then for any $\varepsilon > 0$, we have

$$\mathbb{P} \left(\left| \sum_{i=1}^p v_i \sum_{l=1}^t w_l (X_i(l) - \mu_i(l)) \right| \geq \varepsilon \right) \leq 2 \exp \left(- \frac{3/2\varepsilon^2}{3\rho\|v\|_2^2 + \varepsilon \max_{i=1}^p |v_i| \max_{l=1}^t |w_l|} \right).$$

Lemma 9. Assume that $\{B(u)\}$ is a sequence of adjacency matrices satisfying Assumption 1. For any integer $t \geq 2$, let

$$\begin{aligned} \mathcal{S}(t) &= \{t - s^{j-1}, j = 1, \dots, \lfloor \log(t)/\log(2) \rfloor\}, \quad C > 32 \times 2^{1/4} e^2, \\ \varepsilon_{s,t} &= \sqrt{2 \log \left\{ \frac{t(t+1) \log(t)}{\alpha \log(2)} \right\}}, \quad \tau_{1,s,t} = C\sqrt{n\rho} + \varepsilon_{s,t} \quad \text{and} \quad \tau_{2,s,t} = \sqrt{\frac{(t-s)s}{t}} \rho. \end{aligned}$$

We have that under Assumption 2, the event

$$\mathcal{F}_1 = \left\{ \forall t \geq 2 : \max_{s \in \mathcal{S}(t)} \left\| \text{USVT}(\hat{B}_{s,t}, \tau_{1,s,t}, \tau_{2,s,t}) \right\|_{\text{F}} = 0, t \leq \Delta, \right. \\ \left. \text{and } \max_{s \in \mathcal{S}(t)} \left\| \text{USVT}(\hat{B}_{s,t}, \tau_{1,s,t}, \tau_{2,s,t}) - \hat{\Theta}_{s,t} \right\|_{\text{F}} \leq \sqrt{r} (C\sqrt{n\rho} + \varepsilon_{s,t}), t > \Delta \right\}$$

holds with probability at least $1 - \alpha/2$; under Assumption 3, the event

$$\mathcal{F}_1 = \left\{ \forall t \geq 2 : \max_{s \in \mathcal{S}(t)} \left\| \text{USVT}(\hat{B}_{s,t}, \tau_{1,s,t}, \tau_{2,s,t}) \right\|_{\text{F}} = 0 \right\}$$

holds with probability at least $1 - \alpha/2$.

Proof. Step 1. If Assumption 2 holds, then for $t \leq \Delta$, it holds that

$$\hat{\Theta}_{s,t} = 0 \quad \text{and} \quad \text{rank}(\hat{\Theta}_{s,t}) = 0, \quad \forall s \in \mathcal{S}(t);$$

for $t > \Delta$, it holds that

$$\hat{\Theta}_{s,t} = \begin{cases} (t - \Delta) \sqrt{\frac{s}{t(t-s)}} (\Theta_1 - \Theta_2), & s \leq \Delta, \\ \Delta \sqrt{\frac{t-s}{st}} (\Theta_1 - \Theta_2), & s > \Delta. \end{cases} \quad \text{and} \quad \text{rank}(\hat{\Theta}_{s,t}) \leq r. \quad (9)$$

If Assumption 3 holds, then for any t , it holds that

$$\hat{\Theta}_{s,t} = 0 \quad \text{and} \quad \text{rank}(\hat{\Theta}_{s,t}) = 0, \quad \forall s \in \mathcal{S}(t).$$

Step 2. Due to Definition 2, we have

$$\hat{B}_{s,t} = \sum_{l=1}^t w_l^s B(l),$$

where $\sum_{l=1}^t w_l^s = 0$ and $\sum_{l=1}^t (w_l^s)^2 = 1$.

Define

$$\mathcal{E}_1^c = \left\{ \exists t \geq 2, s \in \mathcal{S}(t) : \|\hat{B}_{s,t} - \hat{\Theta}_{s,t}\|_{\text{op}} > C\sqrt{n\rho} + \varepsilon_{s,t} \right\}.$$

Then it follows from Lemma 5 that,

$$\mathbb{P}(\mathcal{E}_1^c) \leq \sum_{t=2}^{\infty} \frac{\log(t)}{\log(2)} \max_{s \in \mathcal{S}(t)} \mathbb{P} \left\{ \|\hat{B}_{s,t} - \hat{\Theta}_{s,t}\|_{\text{op}} > C\sqrt{n\rho} + \varepsilon_{s,t} \right\} \\ \leq \sum_{t=2}^{\infty} \frac{\log(t)}{\log(2)} \frac{\log(2)}{\log(t)} \frac{\alpha}{t(t+1)} \leq \frac{\alpha}{2},$$

where

$$C > 32 \times 2^{1/4} e^2 \quad \text{and} \quad \varepsilon_{s,t} = \sqrt{2 \log \left\{ \frac{t(t+1) \log(t)}{\alpha \log(2)} \right\}}. \quad (10)$$

Under Assumption 2, it follows from Lemma 6 that $\mathcal{E}_2 \subset \mathcal{E}_1$, where

$$\mathcal{E}_2 = \left\{ \forall t \geq 2 : \max_{s \in \mathcal{S}(t)} \left\| \text{USVT}(\hat{B}_{s,t}, \tau_{1,s,t}, \infty) - \hat{\Theta}_{s,t} \right\|_{\text{F}} \leq \sqrt{r} (C\sqrt{n\rho} + \varepsilon_{s,t}), t > \Delta \right. \\ \left. \text{and } \max_{s \in \mathcal{S}(t)} \left\| \text{USVT}(\hat{B}_{s,t}, \tau_{1,s,t}, \infty) \right\|_{\text{F}} = 0, t \leq \Delta \right\},$$

with C and $\varepsilon_{s,t}$ defined in (10) and

$$\tau_{1,s,t} = C\sqrt{n\rho} + \varepsilon_{s,t}.$$

Due to (9), we have that

$$\left\| \hat{\Theta}_{s,t} \right\|_{\infty} \leq \sqrt{\frac{s(t-s)}{t}} \rho = \tau_{2,s,t}.$$

Therefore, we have that $\mathcal{F}_1 \subset \mathcal{E}_2$.

Under Assumption 3, note that $\hat{\Theta}_{s,t} = 0$ and $\text{rank}(\hat{\Theta}_{s,t}) = 0$. Due to Lemmas 6 and 7, we have $\mathcal{F}_1 \subset \mathcal{E}_1$, which completes the proof. \square

Lemma 10. Assume $\{B(u)\}$ is a sequence of adjacency matrices satisfying Assumption 1. For any integer $t \geq 2$, let

$$\mathcal{S}(t) = \{t - s^{j-1}, j = 1, \dots, \lfloor \log(t)/\log(2) \rfloor\}, \quad C > 32 \times 2^{1/4} e^2, \\ \varepsilon_{s,t} = \sqrt{2 \log \left\{ \frac{2(\gamma+1)^2 \log(\gamma+1)}{\log(2)} \right\}}, \quad \tau_{1,s,t} = C\sqrt{n\rho} + \varepsilon_t \quad \text{and} \quad \tau_{2,s,t} = \sqrt{\frac{(t-s)s}{t}} \rho.$$

We have that under Assumption 2, the event

$$\mathcal{F}_2 = \left\{ \forall t \in \{2, \dots, \gamma+1\} : \max_{s \in \mathcal{S}(t)} \left\| \text{USVT}(\hat{B}_{s,t}, \tau_{1,s,t}, \tau_{2,s,t}) \right\|_{\text{F}} = 0, t \leq \Delta \right. \\ \left. \text{and } \max_{s \in \mathcal{S}(t)} \left\| \text{USVT}(\hat{B}_{s,t}, \tau_{1,s,t}, \tau_{2,s,t}) - \hat{\Theta}_{s,t} \right\|_{\text{F}} \leq \sqrt{r} (C\sqrt{n\rho} + \varepsilon_{s,t}), t > \Delta \right\}$$

holds with probability at least $1 - (\gamma+1)^{-1}/2$; under Assumption 2, the event

$$\mathcal{F}_2 = \left\{ \forall t \in \{2, \dots, \gamma+1\} : \max_{s \in \mathcal{S}(t)} \left\| \text{USVT}(\hat{B}_{s,t}, \tau_{1,s,t}, \tau_{2,s,t}) \right\|_{\text{F}} = 0 \right\}$$

holds with probability at least $1 - (\gamma+1)^{-1}/2$.

Proof. Step 1. If Assumption 2 holds, then for $t \leq \Delta$, it holds that

$$\hat{\Theta}_{s,t} = 0 \quad \text{and} \quad \text{rank}(\hat{\Theta}_{s,t}) = 0, \quad \forall s \in \mathcal{S}(t);$$

for $t > \Delta$, it holds that

$$\hat{\Theta}_{s,t} = \begin{cases} (t - \Delta) \sqrt{\frac{s}{t(t-s)}} (\Theta_1 - \Theta_2), & s \leq \Delta, \\ \Delta \sqrt{\frac{t-s}{st}} (\Theta_1 - \Theta_2), & s > \Delta, \end{cases} \quad \text{and} \quad \text{rank}(\hat{\Theta}_{s,t}) \leq r. \quad (11)$$

In addition, it holds that $\text{rank}(\hat{\Theta}_{s,t}) \leq r$.

If Assumption 3 holds, then for any t , it holds that

$$\hat{\Theta}_{s,t} = 0 \quad \text{and} \quad \text{rank}(\hat{\Theta}_{s,t}) = 0, \quad \forall s \in \mathcal{S}(t).$$

Step 2. Due to Definition 2, we have

$$\hat{B}_{s,t} = \sum_{l=1}^t w_l^s B(l),$$

where $\sum_{l=1}^t w_l^s = 0$ and $\sum_{l=1}^t (w_l^s)^2 = 1$.

Define

$$\mathcal{E}_3^c = \left\{ \exists t \in \{2, \dots, \gamma + 1\}, s \in \mathcal{S}(t) : \|\hat{B}_{s,t} - \hat{\Theta}_{s,t}\|_{\text{op}} > C\sqrt{n\rho} + \varepsilon_{s,t} \right\}.$$

Then it follows from Lemma 5 that,

$$\mathbb{P}(\mathcal{E}_3^c) < \frac{1}{2(\gamma + 1)},$$

where

$$C > 32 \times 2^{1/4} e^2 \quad \text{and} \quad \varepsilon_{s,t} = \sqrt{2 \log \left\{ \frac{2(\gamma + 1)\gamma \log(\gamma + 1)}{\log(2)} \right\}}. \quad (12)$$

Under Assumption 2, it follows from Lemma 6 that $\mathcal{E}_4 \subset \mathcal{E}_3$, where

$$\begin{aligned} \mathcal{E}_4 = & \left\{ \forall t \in \{2, \dots, \gamma + 1\} : \max_{s \in \mathcal{S}(t)} \left\| \text{USVT}(\hat{B}_{s,t}, \tau_{1,s,t}, \infty) - \hat{\Theta}_{s,t} \right\|_{\text{F}} \leq \sqrt{r} (C\sqrt{n\rho} + \varepsilon_{s,t}), t > \Delta \right. \\ & \left. \text{and} \quad \max_{s \in \mathcal{S}(t)} \left\| \text{USVT}(\hat{B}_{s,t}, \tau_{1,s,t}, \infty) \right\|_{\text{F}} = 0, t \leq \Delta \right\}, \end{aligned}$$

with C and $\varepsilon_{s,t}$ defined in (12) and

$$\tau_{1,s,t} = C\sqrt{n\rho} + \varepsilon_{s,t}.$$

Due to (11), we have that

$$\left\| \hat{\Theta}_{s,t} \right\|_{\infty} \leq \sqrt{\frac{s(t-s)}{t}} \rho = \tau_{2,s,t}.$$

Therefore, we have $\mathcal{F}_2 \subset \mathcal{E}_4$.

Under Assumption 3, not that $\hat{\Theta}_{s,t} = 0$ and $\text{rank}(\hat{\Theta}) = 0$. Due to Lemmas 6 and 7, we have $\mathcal{F}_2 \subset \mathcal{E}_3$, which completes the proof. \square

B Proofs of main results

Proof of Theorem 1. We let

$$\tilde{B}_{s,t} = \text{USVT}(\hat{B}_{s,t}, \tau_{1,s,t}, \tau_{2,s,t}), \quad t \geq 2$$

and

$$\mathcal{S}(t) = \{t - 2^{j-1}, j = 1, \dots, \lfloor \log(t)/\log(2) \rfloor\}.$$

The rest of the proof is conducted on the event \mathcal{F}_1 , defined in Lemma 9. In particular,

$$\mathbb{P}\{\mathcal{F}_1\} > 1 - \alpha/2 \quad (13)$$

and the event \mathcal{F}_1 is regarding the data $\{B(t)\}$, which are independent of the data $\{A(t)\}$.

Step 1. Due to Lemma 9, it holds that if Assumption 2 holds and $t \leq \Delta$, or Assumption 3 holds, then $\tilde{B}_{s,t} = 0$, $s \in \mathcal{S}(t)$. Therefore the claim (i) is proved and for the claim (ii), we have

$$\hat{t} - \Delta > 0.$$

Define

$$t_1 = \min \left\{ t > \Delta : \max_{s \in \mathcal{S}(t)} \left[\left\| \left(\hat{A}_{s,t}, \frac{\tilde{B}_{s,t}}{\|\tilde{B}_{s,t}\|_{\mathbb{F}}} \right) \right\| \mathbb{1} \left\{ \|\tilde{B}_{s,t}\|_{\mathbb{F}} > C \log^{1/2}(t/\alpha) \right\} \right] > b_t \right\}. \quad (14)$$

Due to the design of Algorithm 2, we can see that $\hat{t} \leq t_1$ and therefore $d \leq t_1 - \Delta$. In order to provide an upper bound on d , it thus suffices to upper bound t_1 .

Step 2. Recall the quantity

$$\varepsilon_{s,t} = \sqrt{2 \log \left\{ \frac{t(t+1) \log(t)}{\alpha \log(2)} \right\}}$$

defined in Lemma 9. With the quantity $\varepsilon_{s,t}$, we define

$$t_2 = \min \left\{ t > \Delta : \max_{s \in \mathcal{S}(t)} \left[\left\| \left(\hat{A}_{s,t}, \frac{\tilde{B}_{s,t}}{\|\tilde{B}_{s,t}\|_{\mathbb{F}}} \right) \right\| \times \mathbb{1} \left\{ \|\hat{\Theta}_{s,t}\|_{\mathbb{F}} > C \log^{1/2}(t/\alpha) + \sqrt{r} (C\sqrt{n\rho} + \varepsilon_{s,t}) \right\} \right] > b_t \right\}.$$

Due to Lemma 9, we know that if

$$\left\{ \|\hat{\Theta}_{s,t}\|_{\mathbb{F}} > C \log^{1/2}(t/\alpha) + \sqrt{r} (C\sqrt{n\rho} + \varepsilon_{s,t}) \right\}$$

considered in t_2 holds, then

$$\left\{ \|\tilde{B}_{s,t}\|_{\mathbb{F}} > C \log^{1/2}(t/\alpha) \right\}$$

considered in t_1 also holds. This implies that $t_2 > t_1$. It now suffices to find t_2 , which yields an upper bound on d that $d \leq t_2 - \Delta$.

Due to the choices of s , we in turn define

$$J = \min \left\{ j \in \mathbb{N} : \left\| \left(\hat{A}_{\Delta, \Delta+2^j}, \frac{\tilde{B}_{\Delta, \Delta+2^j}}{\|\tilde{B}_{\Delta, \Delta+2^j}\|_{\mathbb{F}}} \right) \right\| \right.$$

$$\times \mathbb{1} \left\{ \|\hat{\Theta}_{\Delta, \Delta+2^j}\|_{\text{F}} > C \log^{1/2}((\Delta + 2^j)/\alpha) + \sqrt{r} (C\sqrt{n\rho} + \varepsilon_{\Delta, \Delta+2^j}) \right\} > b_{\Delta+2^j} \Big\}$$

and $t_3 = \Delta + 2^J$. In the definition of J , we essentially choose the integer pair (s, t) to be $(\Delta, \Delta + 2^J)$. This is to ensure that $s \in \mathcal{S}(t)$ and $s = \Delta$. Due to this construction, we can see that t_3 is an upper bound of t_2 and our task is now to find J defined above.

Step 3. We are now to show that, with a large enough absolute constant $C_d > 0$,

$$J = \left\lceil \log \left(\frac{C_d r \log(\Delta/\alpha)}{\kappa_0^2 n \rho} \right) / \log(2) \right\rceil. \quad (15)$$

For notational simplicity, in the rest of the proof, we assume that

$$\log \left(\frac{C_d r \log(\Delta/\alpha)}{\kappa_0^2 n \rho} \right) / \log(2)$$

is a positive integer. If this is violated, then the proof only needs to be modified by keeping the ceiling operator throughout.

Step 3.1. With J defined in (15), we have that

$$\|\hat{\Theta}_{\Delta, \Delta+2^J}\|_{\text{F}} = \kappa \sqrt{\frac{\Delta \frac{C_d r \log(\Delta/\alpha)}{\kappa_0^2 n \rho}}{\Delta + \frac{C_d r \log(\Delta/\alpha)}{\kappa_0^2 n \rho}}},$$

which can be derived by plugging in Δ and $\Delta + 2^J$ into (11). Due to (2), we have that

$$\|\hat{\Theta}_{\Delta, \Delta+2^J}\|_{\text{F}} > C \log^{1/2}((\Delta + 2^J)/\alpha) + \sqrt{r} (C\sqrt{n\rho} + \varepsilon_{s, \Delta+2^J}). \quad (16)$$

This can be seen in the following three steps.

Step 3.1.1. We first show that

$$3^{-1} \|\hat{\Theta}_{\Delta, \Delta+2^J}\|_{\text{F}} > C \log^{1/2}((\Delta + 2^J)/\alpha). \quad (17)$$

Provided that $C_d < C_{\text{SNR}}$, due to (2), it holds that

$$\|\hat{\Theta}_{\Delta, \Delta+2^J}\|_{\text{F}} \geq \kappa \sqrt{\Delta \frac{C_d r \log(\Delta/\alpha)}{2\kappa_0^2 n \rho}} = \sqrt{\Delta n \rho \frac{C_d r \log(\Delta/\alpha)}{2}}. \quad (18)$$

In addition, provided that $\Delta/\alpha \geq 2$, it holds that

$$\log^{1/2}((\Delta + 2^J)/\alpha) \leq \log^{1/2}(2\Delta/\alpha) \leq \sqrt{2 \log(\Delta/\alpha)}. \quad (19)$$

Therefore, provided that $C_d > 36C^2/\log(2)$ and $n \geq 2$, (17) holds, where $n\rho \geq \log(n)$ assumed in Assumption 1 is used.

Step 3.1.2. Provided that $C_d > 18C^2/\log(2)$, we have that $3^{-1} \|\hat{\Theta}_{\Delta, \Delta+2^J}\|_{\text{F}} > C\sqrt{rn\rho}$, by using (18).

Step 3.1.3. Lastly, we are to show

$$3^{-1} \|\hat{\Theta}_{\Delta, \Delta+2^J}\|_F > C\sqrt{r}\varepsilon_{s, \Delta+2^J} = C\sqrt{2r \log \left\{ \frac{(\Delta + 2^J)(\Delta + 2^J + 1) \log(\Delta + 2^J)}{\alpha \log(2)} \right\}}. \quad (20)$$

Due to (19), the last term in (20) is upper bounded by

$$\begin{aligned} & C\sqrt{2r \log \left\{ \frac{2\Delta(2\Delta + 1) \log(2\Delta)}{\alpha \log(2)} \right\}} \leq C\sqrt{2r \log \left\{ \frac{(2\Delta + 1)^3}{\alpha \log(2)} \right\}} \\ & \leq C\sqrt{8r \log \left\{ \frac{2\Delta}{\alpha} \right\}} \leq C\sqrt{16r \log \left\{ \frac{\Delta}{\alpha} \right\}}. \end{aligned}$$

Therefore provided that $C_d > 288C^2/\log(2)$, (20) holds.

Step 3.2. In addition, we have that

$$\begin{aligned} & \left| \left(\hat{A}_{\Delta, \Delta+2^J}, \frac{\tilde{B}_{\Delta, \Delta+2^J}}{\|\tilde{B}_{\Delta, \Delta+2^J}\|_F} \right) \right| \\ & \geq \left| \left(\hat{\Theta}_{\Delta, \Delta+2^J}, \frac{\tilde{B}_{\Delta, \Delta+2^J}}{\|\tilde{B}_{\Delta, \Delta+2^J}\|_F} \right) \right| - \left| \left(\hat{A}_{\Delta, \Delta+2^J} - \hat{\Theta}_{\Delta, \Delta+2^J}, \frac{\tilde{B}_{\Delta, \Delta+2^J}}{\|\tilde{B}_{\Delta, \Delta+2^J}\|_F} \right) \right| = (I) - (II). \end{aligned} \quad (21)$$

Step 3.2.1. As for (I), we have that

$$\begin{aligned} & \left| \left(\hat{\Theta}_{\Delta, \Delta+2^J}, \frac{\tilde{B}_{\Delta, \Delta+2^J}}{\|\tilde{B}_{\Delta, \Delta+2^J}\|_F} \right) \right| = \|\hat{\Theta}_{\Delta, \Delta+2^J}\|_F \left| \left(\frac{\hat{\Theta}_{\Delta, \Delta+2^J}}{\|\hat{\Theta}_{\Delta, \Delta+2^J}\|_F}, \frac{\tilde{B}_{\Delta, \Delta+2^J}}{\|\tilde{B}_{\Delta, \Delta+2^J}\|_F} \right) \right| \\ & = \frac{\|\hat{\Theta}_{\Delta, \Delta+2^J}\|_F}{2} \left(2 - \left\| \frac{\hat{\Theta}_{\Delta, \Delta+2^J}}{\|\hat{\Theta}_{\Delta, \Delta+2^J}\|_F} - \frac{\tilde{B}_{\Delta, \Delta+2^J}}{\|\tilde{B}_{\Delta, \Delta+2^J}\|_F} \right\|_F^2 \right) \\ & = \frac{\|\hat{\Theta}_{\Delta, \Delta+2^J}\|_F}{2} \left(2 - \left\| \frac{\hat{\Theta}_{\Delta, \Delta+2^J} \|\tilde{B}_{\Delta, \Delta+2^J}\|_F - \tilde{B}_{\Delta, \Delta+2^J} \|\hat{\Theta}_{\Delta, \Delta+2^J}\|_F}{\|\hat{\Theta}_{\Delta, \Delta+2^J}\|_F \|\tilde{B}_{\Delta, \Delta+2^J}\|_F} \right\|_F^2 \right) \\ & \geq \frac{\|\hat{\Theta}_{\Delta, \Delta+2^J}\|_F}{2} \left(2 - \left\| \frac{\hat{\Theta}_{\Delta, \Delta+2^J} - \tilde{B}_{\Delta, \Delta+2^J}}{\|\hat{\Theta}_{\Delta, \Delta+2^J}\|_F} + \frac{\|\hat{\Theta}_{\Delta, \Delta+2^J}\|_F - \|\tilde{B}_{\Delta, \Delta+2^J}\|_F}{\|\hat{\Theta}_{\Delta, \Delta+2^J}\|_F} \right\|_F^2 \right) \\ & \geq \frac{\|\hat{\Theta}_{\Delta, \Delta+2^J}\|_F}{2} \left\{ 2 - 4 \left(\frac{\|\hat{\Theta}_{\Delta, \Delta+2^J} - \tilde{B}_{\Delta, \Delta+2^J}\|_F}{\|\hat{\Theta}_{\Delta, \Delta+2^J}\|_F} \right)^2 \right\} \\ & \geq \frac{\|\hat{\Theta}_{\Delta, \Delta+2^J}\|_F}{2} \left\{ 2 - 4 \left(\frac{C\sqrt{rn\rho} + C\sqrt{r}\varepsilon_{\Delta, \Delta+2^J}}{\|\hat{\Theta}_{\Delta, \Delta+2^J}\|_F} \right)^2 \right\} \geq \frac{\|\hat{\Theta}_{\Delta, \Delta+2^J}\|_F}{2}, \end{aligned} \quad (22)$$

where the third inequality is due to the event \mathcal{F}_1 and the last inequality follows from (16) with a sufficiently large C_{SNR} .

Step 3.2.2. As for (II), due to the independence between $\{A(t)\}$ and $\{B(t)\}$, it follows from Lemma 8 and (16) that

$$\begin{aligned} & \mathbb{P}_A \left\{ \left| \left(\hat{A}_{\Delta, \Delta+2^J} - \hat{\Theta}_{\Delta, \Delta+2^J}, \frac{\tilde{B}_{\Delta, \Delta+2^J}}{\|\tilde{B}_{\Delta, \Delta+2^J}\|_{\text{F}}} \right) \right| \geq b_{\Delta+2^J} \right\} \\ & \leq \exp \left\{ - \frac{3/2b_t^2}{3\rho + b_{\Delta+2^J}\rho C^{-1} \log^{-1/2}((\Delta + 2^J)/\alpha)} \right\} < \frac{\alpha}{2}. \end{aligned} \quad (23)$$

To be specific, the CUSUM weights are regarded as the $\{w_l\}$ sequence in Lemma 8 and all the entries in $\tilde{B}_{\Delta, \Delta+2^J} \|\tilde{B}_{\Delta, \Delta+2^J}\|_{\text{F}}^{-1}$ are regarded as the $\{v_i\}$ sequence in Lemma 8. Therefore, $\|v\|_2 = 1$, $\max_{l=1}^t |w_l| \leq 2^{-J/2}$ and

$$\max_{i=1}^p |v_i| \leq \frac{\rho \sqrt{\frac{2^J \Delta}{\Delta+2^J}}}{C \log^{1/2}((\Delta + 2^J)/\alpha)} \leq \frac{\rho 2^{J/2}}{C \log^{1/2}((\Delta + 2^J)/\alpha)},$$

where the last inequality follows from (16) and the definition of \mathcal{F}_1 .

Due to (16), with a sufficiently large C_{SNR} , it holds that

$$\frac{\|\hat{\Theta}_{\Delta, \Delta+2^J}\|_{\text{F}}}{2} > 2b_{\Delta+2^J}.$$

Then, combining (21), (22) and (23), it holds that

$$\mathbb{P}_A \left\{ \left| \left(\hat{A}_{\Delta, \Delta+2^J}, \frac{\tilde{B}_{\Delta, \Delta+2^J}}{\|\tilde{B}_{\Delta, \Delta+2^J}\|_{\text{F}}} \right) \right| \geq b_{\Delta+2^J} \right\} > 1 - \frac{\alpha}{2}. \quad (24)$$

Step 3.3. Combining (13) and (24), we have that

$$\mathbb{P} \left\{ \left| \left(\hat{A}_{\Delta, \Delta+2^J}, \frac{\tilde{B}_{\Delta, \Delta+2^J}}{\|\tilde{B}_{\Delta, \Delta+2^J}\|_{\text{F}}} \right) \right| \geq b_{\Delta+2^J} \mid \mathbb{1} \left\{ \|\tilde{B}_{\Delta, \Delta+2^J}\|_{\text{F}} > C \log^{1/2}((\Delta + 2^J)/\alpha) \right\} > b_{\Delta+2^J} \right\} > 1 - \alpha,$$

which completes the proof. □

Proof of Corollary 2. We let

$$\tilde{B}_{s,t} = \text{USVT}(\hat{B}_{s,t}, \tau_{1,s,t}, \tau_{2,s,t}), \quad t > N.$$

Let

$$\mathcal{S}(t) = \{t - 2^{j-1}, j = 1, \dots, \lfloor \log(t)/\log(2) \rfloor\}.$$

Step 1. Due to Lemma 10, it holds that if Assumption 3 holds, then with probability at least $1 - (\gamma + 1)^{-1}$, the event \mathcal{F}_2 holds, i.e. $\tilde{B}_{s,t} = 0$, for all $t \in \{2, \dots, \gamma + 1\}$ and $s \in \mathcal{S}(t)$. Then we have

$$\mathbb{E}_\infty(\hat{t}) = \sum_{t=1}^{\infty} \mathbb{P}(\hat{t} \geq t) \geq \sum_{t=1}^{\gamma+1} \mathbb{P}(\hat{t} \geq t) \geq (\gamma + 1) \mathbb{P}(\hat{t} \geq \gamma + 1) \geq (\gamma + 1) \left(1 - \frac{1}{\gamma + 1}\right) = \gamma.$$

The claim (i) is proved.

Step 2. As for the claim (ii), recall the event \mathcal{F}_2 and associated quantities defined in Lemma 10. We have that $\mathbb{P}(\mathcal{F}_2) > 1 - 1/\{2(\gamma + 1)\}$. Conditional on the event \mathcal{F}_2 instead of \mathcal{F}_1 , the rest of the proof is identical to that of Theorem 1. \square

Proof of Corollary 4. The proof is almost identical to the proof of Theorem 1, except that the large probability events where USVT estimators are well controlled in the proof of Theorem 1 are replaced by Theorem 2.1 in Gao et al. (2015). In fact, Theorem 2.1 in Gao et al. (2015) is stated and proved by assuming $\rho = 1$. In order to get an upper bound being a function of ρ , we only need to change Lemmas 4.1-4.3 in Gao et al. (2015) correspondingly. \square

Proof of Proposition 3. This proof consists of two different cases: a) $r \lesssim \sqrt{n}$ and b) $r \gtrsim \sqrt{n}$.

Case 1: $r \lesssim \sqrt{n}$.

Step 1 - Setup. We assume the networks are generated as follows. Prior to the change point, if there exists any, the adjacency matrices are generated independently from the distribution P_0 , which has the graphon matrix

$$\Theta_1 = (\rho/2)_{i,j=1}^n.$$

If there exists a change point, then the adjacency matrices after the change point are generated independently from the distribution

$$P_1 = \frac{1}{2^n} \sum_{u \in \{\pm 1\}^n} P_{1,u},$$

where the graphon of the distribution $P_{1,u}$ is $\rho/2 \mathbb{1} \mathbb{1}^\top + \kappa_0 \rho u u^\top$, $u \in \{\pm 1\}^n$.

For any $M \in \mathbb{N}$, let P^M be the restriction of a distribution P on \mathcal{F}_M , i.e. the σ -field generated by the observations $\{A(t)\}_{t=1}^M$. For notational simplicity, in this proof, the adjacency matrices $A(t)$'s will be denoted as A^t 's. For any $\nu \geq 1$ and $M \geq \nu$, we have that for any $M \geq \Delta$, let

$$Z_{\nu,M} = \log \left(\frac{P_{\kappa_0,\nu}^M}{P_{\kappa_0,\infty}^M} \right),$$

where $P_{\kappa,\infty}$ indicates the distribution under which there is no change point.

Step 2 - When $Z_{\nu,T}$ is upper bounded. For any $\nu \geq 1$, define the event

$$\mathcal{E}_\nu = \left\{ \nu < T < \nu + \frac{\log(1/\alpha)}{8\kappa_0^2 n \rho}, \quad Z_{\nu,T} < \frac{3}{4} \log(1/\alpha) \right\}.$$

Then we have

$$\mathbb{P}_{\kappa,\nu}(\mathcal{E}_\nu) = \frac{P_{\kappa_0,\nu}(\mathcal{E}_\nu)}{P_{\kappa,\infty}(\mathcal{E}_\nu)} \leq \alpha^{-3/4} \alpha = \alpha^{1/4}, \quad (25)$$

where the inequality follows from the definition of \mathcal{D} and \mathcal{E}_ν .

Step 3 - When $Z_{\nu,T}$ is lower bounded. For any $\nu \geq 1$ and $T \in \mathcal{D}$, since $\{T \geq \nu\} \in \mathcal{F}_{\nu-1}$, we have that

$$\begin{aligned}
& \mathbb{P}_{\kappa,\nu} \left\{ \nu < T < \nu + \frac{\log(1/\alpha)}{8\kappa_0^2 n \rho}, \quad Z_{\nu,T} \geq \frac{3}{4} \log(1/\alpha) \middle| T \geq \nu \right\} \\
& \leq \text{ess sup } \mathbb{P}_{\kappa,\nu} \left\{ \max_{1 \leq l \leq \frac{\log(1/\alpha)}{8\kappa_0^2 n \rho}} Z_{\nu,\nu+l} \geq \frac{3}{4} \log(1/\alpha) \middle| A^1, \dots, A^\nu \right\} \\
& \leq \frac{\log(1/\alpha)}{8\kappa_0^2 n \rho} \max_{1 \leq l \leq \frac{\log(1/\alpha)}{8\kappa_0^2 n \rho}} \text{ess sup } \mathbb{P}_{\kappa,\nu} \left\{ Z_{\nu,\nu+l} \geq \frac{3}{4} \log(1/\alpha) \middle| A^1, \dots, A^\nu \right\} \\
& \leq \frac{\frac{\log(1/\alpha)}{8\kappa_0^2 n \rho}}{\exp \left\{ \frac{3}{4} \log(1/\alpha) \right\}} \max_{1 \leq l \leq \frac{\log(1/\alpha)}{8\kappa_0^2 n \rho}} \text{ess sup } \mathbb{E}_{\kappa,\nu} \left\{ \exp(Z_{\nu,\nu+l}) \middle| A^1, \dots, A^\nu \right\}. \tag{26}
\end{aligned}$$

Step 3.1. Note that for any $l \in \{1, \dots, \log(1/\alpha)(8\kappa_0^2 n \rho)^{-1}\}$, it holds that

$$\mathbb{E}_{\kappa,\nu} \left\{ \exp(Z_{\nu,\nu+l}) \middle| A^1, \dots, A^\nu \right\} = \mathbb{E}_{\kappa,\nu} \left\{ \left(\frac{P_{\kappa_0,\nu}^{\nu+l}}{P_{\kappa_0,\infty}^{\nu+l}} \right) \middle| A^1, \dots, A^\nu \right\}. \tag{27}$$

In addition, letting $\zeta = \rho/2$ and v_i be the i th entry of any vector v , we have that

$$\begin{aligned}
& \mathbb{E}_{P_1} \left(\frac{P_1}{P_0}(A) \right) = \mathbb{E}_u \mathbb{E}_{A|u} \left(\frac{1}{2^n} \sum_{v \in \{\pm 1\}} \frac{P_{1,v}}{P_0}(A) \right) \\
& = \mathbb{E}_u \mathbb{E}_{A|u} \left\{ \frac{1}{2^n} \sum_{v \in \{\pm 1\}} \prod_{1 \leq i < j \leq n} \left(\frac{\zeta + \kappa_0 \rho v_i v_j}{\zeta} \right)^{A_{ij}} \left(\frac{1 - \zeta - \kappa_0 \rho v_i v_j}{1 - \zeta} \right)^{1 - A_{ij}} \right\} \\
& = \mathbb{E}_u \left\{ \frac{1}{2^n} \sum_{v \in \{\pm 1\}} \prod_{1 \leq i < j \leq n} \left\{ 1 + \frac{\kappa_0^2 \rho^2 u_i u_j v_i v_j}{\zeta(1 - \zeta)} \right\} \right\} \\
& \leq \mathbb{E}_u \left\{ \frac{1}{2^n} \sum_{v \in \{\pm 1\}} \prod_{i,j=1}^n \left\{ 1 + \frac{\kappa_0^2 \rho^2 u_i u_j v_i v_j}{\zeta(1 - \zeta)} \right\} \right\}, \tag{29}
\end{aligned}$$

where in (29), u is a random vector with entries being independent Rademacher random variables. We further have that

$$(29) \leq \mathbb{E}_u \mathbb{E}_v \prod_{i,j=1}^n \exp \left\{ \frac{\kappa_0^2 \rho^2 u_i u_j v_i v_j}{\zeta(1 - \zeta)} \right\} = \mathbb{E}_{u,v} \exp \left\{ \frac{4\kappa_0^2 \rho}{2 - \rho} (u^\top v)^2 \right\}, \tag{30}$$

where u and v are independent random vectors with entries being independent Rademacher random variables. Finally, we have that

$$(30) = \mathbb{E}_u \exp \left\{ \frac{4\kappa_0^2 \rho}{2 - \rho} (u^\top 1)^2 \right\}, \tag{31}$$

where $\mathbf{1}$ is an all-one n -dimensional vector. Equation (31) is due to the fact that for each $i \in \{1, \dots, n\}$, $u_i v_i$ has the same distribution as u_i .

Step 3.2. Let

$$\varepsilon_n = \left(\frac{\sum_{i=1}^n u_i}{n} \right)^2.$$

Then we have that for any $x > 0$, due to Hoeffding's inequality that

$$\mathbb{P}\{\varepsilon_n > x\} \leq 2 \exp(-2nx).$$

Therefore

$$\begin{aligned} \mathbb{E}_u \exp \left\{ \frac{4\kappa_0^2 n^2 \rho}{2-\rho} (u^\top \mathbf{1})^2 \right\} &= \int_0^\infty \mathbb{P} \left\{ \exp \left(\frac{4\kappa_0^2 n^2 \rho}{2-\rho} \varepsilon_n \right) > x \right\} dx \\ &\leq 1 + \int_1^\infty \mathbb{P} \left\{ \varepsilon_n > \log(x) \frac{2-\rho}{4\kappa_0^2 n^2 \rho} \right\} dx \leq 1 + 2 \int_1^\infty \exp \left\{ \log(x) \frac{\rho-2}{2\kappa_0^2 n \rho} \right\} dx \\ &\leq 1 + \frac{2}{1 + \frac{\rho-2}{2\kappa_0^2 n \rho}} x^{1 + \frac{\rho-2}{2\kappa_0^2 n \rho}} \Big|_1^\infty = 1 - \frac{2}{1 + \frac{\rho-2}{2\kappa_0^2 n \rho}} \leq \exp(4\kappa_0^2 n \rho), \end{aligned} \quad (32)$$

provided that

$$\rho + 2\kappa_0^2 n \rho < 1. \quad (33)$$

Step 3.3. Combining (26), (27), (31) and (32), we have that

$$\begin{aligned} \mathbb{P}_{\kappa, \nu} \left\{ \nu < T < \nu + \frac{\log(1/\alpha)}{8\kappa_0^2 n \rho}, \quad Z_{\nu, T} \geq \frac{3}{4} \log(1/\alpha) \middle| T \geq \nu \right\} \\ \leq \frac{\log(1/\alpha)}{8\kappa_0^2 n \rho} \frac{\exp \left\{ \frac{\log(1/\alpha)}{8\kappa_0^2 n \rho} 4\kappa_0^2 n \rho \right\}}{\exp \left\{ \frac{3}{4} \log(1/\alpha) \right\}} \leq \alpha^{1/8}, \end{aligned} \quad (34)$$

provided that

$$\alpha^{1/8} \log(1/\alpha) < 8\kappa_0^2 n \rho. \quad (35)$$

Step 4. Combining (41) and (34), we then have

$$\sup_{\nu \geq 1} \mathbb{P}_{\kappa, \nu} \left\{ \nu < T < \nu + \frac{\log(1/\alpha)}{8\kappa_0^2 n \rho} \right\} \leq 2\alpha^{1/8}.$$

Then it holds that

$$\begin{aligned} \mathbb{E}_{\kappa, \Delta} \{(T - \Delta)_+\} &\geq \frac{\log(1/\alpha)}{8\kappa_0^2 n \rho} \mathbb{P}_{\kappa, \nu} \left\{ T - \Delta \geq \frac{\log(1/\alpha)}{8\kappa_0^2 n \rho} \right\} \\ &= \frac{\log(1/\alpha)}{8\kappa_0^2 n \rho} \mathbb{P}_{\kappa, \nu} \left[\mathbb{P}_{\kappa, \nu} \{T > \Delta\} - \mathbb{P}_{\kappa, \nu} \left\{ \Delta < T < \Delta + \frac{\log(1/\alpha)}{8\kappa_0^2 n \rho} \right\} \right] \\ &\geq \frac{\log(1/\alpha)}{8\kappa_0^2 n \rho} (1 - \alpha - 2\alpha^{1/8}) \geq \frac{\log(1/\alpha)}{16\kappa_0^2 n \rho}, \end{aligned}$$

provided that

$$\alpha + 2\alpha^{1/8} < 1/2. \quad (36)$$

Step 5. Finally, we are to show the set of parameters satisfying (33), (35) and (49) is not an empty set. For instance, we take $\rho = 1/4$ and $\kappa_0^2 n = 1/2$, then (33) holds. With this choice, (35) holds if

$$\alpha^{1/8} < 1/\log(1/\alpha) \quad (37)$$

holds. Since $\alpha < \alpha^{1/8}$, (49) holds if

$$\alpha^{1/8} < 1/6 \quad (38)$$

holds. The choice of $\alpha = 30^{-8}$ satisfies both (37) and (38).

Step 6. We have now shown that when $r \lesssim \sqrt{n}$, it holds that

$$\inf_{\hat{t} \in \mathcal{D}} \sup_{P_{\kappa, \Delta}} \mathbb{E}_P \{(\hat{t} - \Delta)_+\} \geq \frac{c \log(1/\alpha)}{\kappa_0^2 n \rho}, \quad (39)$$

with an absolute constant $c > 0$.

Case 2: $r \gtrsim \sqrt{n}$.

Step 1 - Setup. We assume that the networks are generated as follows. Prior to the change point, if there exists any, the adjacency matrices are generated independently from the distribution P_0 , which has the graphon matrix

$$\Theta_0 = (\rho/2)_{i,j=1}^n.$$

If there exists a change point, then the adjacency matrices after the change point are generated independently from the distribution

$$P_1 = \frac{1}{2^{(r^2/2)}} \sum_{Z \in \mathcal{Z}} P_{1,Z},$$

where the graphon of the distribution $P_{1,Z}$ is $\rho/2 \mathbb{1} \mathbb{1}^\top + \kappa_0 \rho n / r Z$ and the collection \mathcal{Z} is the set for all symmetric matrices satisfying $Z_{ij} = 0$, if $\max\{i, j\} > r$, and all the upper triangular matrix of $Z_{(1:r), (1:r)}$ are independent Radamacher random variables.

In order to show that P_1 is a probability distribution, it suffices to justify that for any $Z \in \mathcal{Z}$, $P_{1,Z}$ is a suitable probability distribution.

- Firstly, we have that

$$\|\kappa_0 \rho n / r Z\|_F = \kappa_0 \rho n.$$

- Secondly, we have that the entries of the matrix Z are all in the set $\{0, \pm 1\}$. This means that provided

$$\kappa_0 n / r < 1/2, \quad (40)$$

all the entries of $P_{1,Z,E}$ are in the interval $[0, \rho]$.

- Lastly, the rank of the matrix Z is upper bounded by r .

For any $M \in \mathbb{N}$, let P^M be the restriction of a distribution P on \mathcal{F}_M , i.e. the σ -field generated by the observations $\{A(t)\}_{t=1}^M$. For notational simplicity, in this proof, the adjacency matrices $A(t)$'s will be denoted as A^t 's. For any $\nu \geq 1$ and $M \geq \nu$, we have that for any $M \geq \Delta$, let

$$Z_{\nu,M} = \log \left(\frac{P_{\kappa_0,\nu}^M}{P_{\kappa_0,\infty}^M} \right),$$

where $P_{\kappa,\infty}$ indicates the distribution under which there is no change point.

Step 2 - When $Z_{\nu,T}$ is upper bounded. For any $\nu \geq 1$, define the event

$$\mathcal{E}_\nu = \left\{ \nu < T < \nu + \frac{r^2/n \log(1/\alpha)}{8\kappa_0^2 n \rho}, \quad Z_{\nu,T} < \frac{3}{4} \log(1/\alpha) \right\}.$$

Then we have

$$\mathbb{P}_{\kappa,\nu}(\mathcal{E}_\nu) = \frac{P_{\kappa_0,\nu}(\mathcal{E}_\nu)}{P_{\kappa,\infty}(\mathcal{E}_\nu)} \leq \alpha^{-3/4} \alpha = \alpha^{1/4}, \quad (41)$$

where the inequality follows from the definition of \mathcal{D} and \mathcal{E}_ν .

Step 3 - When $Z_{\nu,T}$ is lower bounded. For any $\nu \geq 1$ and $T \in \mathcal{D}$, since $\{T \geq \nu\} \in \mathcal{F}_{\nu-1}$, we have that

$$\begin{aligned} & \mathbb{P}_{\kappa,\nu} \left\{ \nu < T < \nu + \frac{r^2/n \log(1/\alpha)}{8\kappa_0^2 n \rho}, \quad Z_{\nu,T} \geq \frac{3}{4} \log(1/\alpha) \middle| T \geq \nu \right\} \\ & \leq \text{ess sup } \mathbb{P}_{\kappa,\nu} \left\{ \max_{1 \leq l \leq \frac{r^2/n \log(1/\alpha)}{8\kappa_0^2 n \rho}} Z_{\nu,\nu+l} \geq \frac{3}{4} \log(1/\alpha) \middle| A^1, \dots, A^\nu \right\} \\ & \leq \frac{r^2/n \log(1/\alpha)}{8\kappa_0^2 n \rho} \max_{1 \leq l \leq \frac{r^2/n \log(1/\alpha)}{8\kappa_0^2 n \rho}} \text{ess sup } \mathbb{P}_{\kappa,\nu} \left\{ Z_{\nu,\nu+l} \geq \frac{3}{4} \log(1/\alpha) \middle| A^1, \dots, A^\nu \right\} \\ & \leq \frac{\frac{r^2/n \log(1/\alpha)}{8\kappa_0^2 n \rho}}{\exp \left\{ \frac{3}{4} \log(1/\alpha) \right\}} \max_{1 \leq l \leq \frac{r^2/n \log(1/\alpha)}{8\kappa_0^2 n \rho}} \text{ess sup } \mathbb{E}_{\kappa,\nu} \left\{ \exp(Z_{\nu,\nu+l}) \middle| A^1, \dots, A^\nu \right\}. \end{aligned} \quad (42)$$

Step 2.1. Note that for any $l \in \{1, \dots, r^2/n \log(1/\alpha)(8\kappa_0^2 n \rho)^{-1}\}$, it holds that

$$\mathbb{E}_{\kappa,\nu} \left\{ \exp(Z_{\nu,\nu+l}) \middle| A^1, \dots, A^\nu \right\} = \mathbb{E}_{\kappa,\nu} \left\{ \left(\frac{P_{\kappa_0,\nu}^{\nu+l}}{P_{\kappa_0,\infty}^{\nu+l}} \right) \middle| A^1, \dots, A^\nu \right\}. \quad (43)$$

In addition, letting $\zeta = \rho/2$, $U_{ij} = \kappa_0 \rho n / r Z_{ij}$ and $V_{ij} = \kappa_0 \rho n / r W_{ij}$, we have that

$$\begin{aligned} & \mathbb{E}_{P_1} \left(\frac{P_1}{P_0} \right) = \mathbb{E}_Z \mathbb{E}_{A|Z} \left(\frac{1}{2^{(r^2/2)}} \sum_{W \in \mathcal{Z}} \frac{P_{1,W}}{P_0} \right) \\ & = \mathbb{E}_Z \mathbb{E}_{A|Z} \left\{ \frac{1}{2^{(r^2/2)}} \sum_{W \in \mathcal{Z}} \prod_{1 \leq i < j \leq n} \left(\frac{\zeta + V_{ij}}{\zeta} \right)^{A_{ij}} \left(\frac{1 - \zeta - V_{ij}}{1 - \zeta} \right)^{1 - A_{ij}} \right\} \end{aligned}$$

$$\begin{aligned}
&= \mathbb{E}_Z \left\{ \frac{1}{2^{(r^2/2)}} \sum_{W \in \mathcal{Z}} \prod_{1 \leq i < j \leq n} \left\{ 1 + \frac{U_{ij} V_{ij}}{\zeta(1-\zeta)} \right\} \right\} \\
&\leq \mathbb{E}_Z \left\{ \frac{1}{2^{(r^2/2)}} \sum_{W \in \mathcal{Z}} \prod_{i,j=1}^n \left\{ 1 + \frac{U_{ij} V_{ij}}{\zeta(1-\zeta)} \right\} \right\} \\
&\leq \mathbb{E}_Z \mathbb{E}_W \prod_{i,j=1}^n \exp \left\{ \frac{U_{ij} V_{ij}}{\zeta(1-\zeta)} \right\} = \mathbb{E}_Z \mathbb{E}_W \exp \left\{ \frac{\kappa_0^2 \rho n^2 / r^2}{2-\rho} \langle Z, W \rangle \right\}. \tag{44}
\end{aligned}$$

Step 2.2 For any fixed $Z, W \in \mathcal{Z}$, it holds that

$$\langle Z, W \rangle = 2z^\top w, \tag{45}$$

where z and w are vectorised upper triangular parts of Z and W , respectively. The vectors z and w are all $r^2/2$ -dimensional vectors, consisting of only ± 1 .

Step 2.3. Due to (45), it holds that

$$\mathbb{E}_{P_1} \left(\frac{P_1}{P_0} \right) \leq \mathbb{E}_Z \mathbb{E}_W \exp \left\{ \frac{2\kappa_0^2 \rho n^2 / r^2}{2-\rho} (z^\top w) \right\} = \mathbb{E}_Z \exp \left\{ \frac{2\kappa_0^2 \rho n^2 / r^2}{2-\rho} (z^\top 1) \right\}.$$

Let

$$\varepsilon = \frac{\sum_{i=1}^{r^2/2} z_i}{r^2/2}.$$

Then we have that for any $x > 1$, due to Hoeffding's inequality that

$$\mathbb{P} \{ \varepsilon > x \} \leq \exp(-2x^2 r^2) \leq \exp(-2xr^2).$$

We have that

$$\begin{aligned}
&\mathbb{E}_Z \exp \left\{ \frac{2\kappa_0^2 \rho n^2 / r^2}{2-\rho} (z^\top 1) \right\} = \int_0^\infty \mathbb{P} \left\{ \exp \left(\frac{\kappa_0^2 \rho n^2}{2-\rho} \varepsilon_n \right) > x \right\} dx \\
&\leq a + \int_a^\infty \mathbb{P} \left\{ \varepsilon_n > \log(x) \frac{2-\rho}{\kappa_0^2 \rho n^2} \right\} dx \leq a + \int_a^\infty \exp \left\{ -\log(x) \frac{2r^2(2-\rho)}{\kappa_0^2 n^2 \rho} \right\} dx \\
&\leq a - \frac{1}{1 - \frac{2r^2(2-\rho)}{\kappa_0^2 n^2 \rho}} = a + \frac{\kappa_0^2 n^2 \rho}{2r^2 - \kappa_0^2 n^2 \rho} \leq a + \frac{\kappa_0^2 n^2 \rho}{r^2},
\end{aligned}$$

provided that

$$\kappa_0^2 n^2 \rho < r^2, \tag{46}$$

where

$$a = \exp \left\{ \frac{2-\rho}{\kappa_0^2 \rho n^2} \right\}.$$

Then we have

$$\mathbb{E}_{P_1} \left(\frac{P_1}{P_0} \right) \leq \exp \left\{ \frac{2-\rho}{\kappa_0^2 \rho n^2} \right\} \left\{ 1 + \exp \left\{ \frac{\rho-2}{\kappa_0^2 \rho n^2} \right\} \frac{\kappa_0^2 n^2 \rho}{r^2} \right\} \leq \exp \left\{ \frac{2-\rho}{\kappa_0^2 \rho n^2} \right\} \exp \left\{ \frac{\kappa_0^2 n^2 \rho}{r^2} \right\}. \tag{47}$$

Step 3. Combining (42), (43) and (47), we then have

$$\begin{aligned} & \mathbb{P}_{\kappa,\nu} \left\{ \nu < T < \nu + \frac{r^2/n \log(1/\alpha)}{8\kappa_0^2 n \rho}, \quad Z_{\nu,T} \geq \frac{3}{4} \log(1/\alpha) \middle| T \geq \nu \right\} \\ & \leq \frac{\frac{r^2/n \log(1/\alpha)}{8\kappa_0^2 n \rho}}{\exp \left\{ \frac{3}{4} \log(1/\alpha) \right\}} \exp \left\{ \frac{r^2/n \log(1/\alpha)}{8\kappa_0^2 n \rho} \frac{2-\rho}{\kappa_0^2 \rho n^2} \right\} \exp \left\{ \frac{r^2/n \log(1/\alpha)}{8\kappa_0^2 n \rho} \frac{\kappa_0^2 n^2 \rho}{r^2} \right\} \\ & \leq \alpha^{3/4} \alpha^{-1/8} \alpha^{-1/8} \alpha^{-1/8} \leq \alpha^{1/4}, \end{aligned}$$

provided that

$$\frac{r \log(1/\alpha)}{8\kappa_0^2 n^2 \rho} \leq \alpha^{-1/8} \quad \text{and} \quad \frac{r^2}{8\kappa_0^4 n^4 \rho^2} \leq 1/8. \quad (48)$$

Then it holds that

$$\begin{aligned} & \mathbb{E}_{\kappa,\Delta} \{ (T - \Delta)_+ \} \geq \frac{r^2/n \log(1/\alpha)}{8\kappa_0^2 n \rho} \mathbb{P}_{\kappa,\nu} \left\{ T - \Delta \geq \frac{r^2/n \log(1/\alpha)}{8\kappa_0^2 n \rho} \right\} \\ & = \frac{r^2/n \log(1/\alpha)}{8\kappa_0^2 n \rho} \mathbb{P}_{\kappa,\nu} \left[\mathbb{P}_{\kappa,\nu} \{ T > \Delta \} - \mathbb{P}_{\kappa,\nu} \left\{ \Delta < T < \Delta + \frac{r^2/n \log(1/\alpha)}{8\kappa_0^2 n \rho} \right\} \right] \\ & \geq \frac{r^2/n \log(1/\alpha)}{8\kappa_0^2 n \rho} (1 - \alpha - 2\alpha^{1/4}) \geq \frac{r^2/n \log(1/\alpha)}{16\kappa_0^2 n \rho}, \end{aligned}$$

provided that

$$\alpha + 2\alpha^{1/4} < 1/2. \quad (49)$$

Step 4. Finally, we are to show the set of parameters satisfying (40), (46), (48) and (49) is not an empty set. For instance, we take $\rho = 1/5$, $r = 30$ and $\kappa_0 n = 14$, then (40), (46) and the second condition in (48) hold. With this choice, the first half of (48) and (49) hold with the choice of $\alpha = 1/2000$. This shows that the choice is not empty. In addition, provided that $n \leq 900$, we have that $r \geq \sqrt{n}$.

Step 5. We have now shown that when $r \gtrsim \sqrt{n}$, it holds that

$$\inf_{\hat{t} \in \mathcal{D}} \sup_{P_{\kappa,\Delta}} \mathbb{E}_P \{ (\hat{t} - \Delta)_+ \} \geq \frac{c \log(1/\alpha) r^2/n}{\kappa_0^2 n \rho}, \quad (50)$$

with an absolute constant $c > 0$.

Finally, combining (39) and (50), we conclude the proof. \square

References

- AUE, A. and HORVÁTH, L. (2004). Delay time in sequential detection of change. *Statistics & Probability Letters*, **67** 221–231.
- CHATTERJEE, S. (2015). Matrix estimation by universal singular value thresholding. *The Annals of Statistics*, **43** 177–214.

- CHEN, H. (2019). Sequential change-point detection based on nearest neighbors. *The Annals of Statistics*, **47** 1381–1407.
- CHEN, H. and CHU, L. (2019). *gStream: Graph-Based Sequential Change-Point Detection for Streaming Data*. R package version 0.2.0, URL <https://CRAN.R-project.org/package=gStream>.
- CHEN, Y., WANG, T. and SAMWORTH, R. J. (2020). High-dimensional, multiscale online change-point detection. *arXiv preprint arXiv:2003.03668*.
- CHU, C.-S. J., STINCHCOMBE, M. and WHITE, H. (1996). Monitoring structural change. *Econometrica: Journal of the Econometric Society* 1045–1065.
- DETTE, H. and GÖSMANN, J. (2019). A likelihood ratio approach to sequential change point detection for a general class of parameters. *Journal of the American Statistical Association* 1–17.
- EAGLE, N. and PENTLAND, A. S. (2006). Reality mining: sensing complex social systems. *Personal and ubiquitous computing*, **10** 255–268.
- GAO, C., LU, Y. and ZHOU, H. H. (2015). Rate-optimal graphon estimation. *The Annals of Statistics*, **43** 2624–2652.
- HE, X., XIE, Y., WU, S.-M. and LIN, F.-C. (2018). Sequential graph scanning statistic for change-point detection. In *2018 52nd Asilomar Conference on Signals, Systems, and Computers*. IEEE, 1317–1321.
- HOLLAND, P. W., LASKEY, K. B. and LEINHARDT, S. (1983). Stochastic blockmodels: First steps. *Social Networks* 109–137.
- JAMES, N. A., ZHANG, W. and MATTESON, D. S. (2019). ecp: An R package for nonparametric multiple change point analysis of multivariate data. r package version 3.1.2. URL <https://cran.r-project.org/package=ecp>.
- KARRER, B. and NEWMAN, M. E. (2011). Stochastic blockmodels and community structure in networks. *Physical review E*, **83** 016107.
- KESHAVERZ, H. and MICHAELIDIS, G. (2020). Online detection of local abrupt changes in high-dimensional gaussian graphical models. *arXiv preprint arXiv:2003.06961*.
- KESHAVERZ, H., MICHAELIDIS, G. and ATCHADE, Y. (2018). Sequential change-point detection in high-dimensional gaussian graphical models. *arXiv preprint arXiv:1806.07870*.
- KIRCH, C. (2008). Bootstrapping sequential change-point tests. *Sequential Analysis*, **27** 330–349.
- LAI, T. L. (1981). Asymptotic optimality of invariant sequential probability ratio tests. *The Annals of Statistics* 318–333.
- LAI, T. L. (1998). Information bounds and quick detection of parameter changes in stochastic systems. *IEEE Transactions on Information Theory*, **44** 2917–2929.
- LAI, T. L. (2001). Sequential analysis: some classical problems and new challenges. *Statistica Sinica* 303–351.

- LOH, P.-L. and WAINWRIGHT, M. J. (2013). Regularized m-estimators with nonconvexity: Statistical and algorithmic theory for local optima. In *Advances in Neural Information Processing Systems*. 476–484.
- LORDEN, G. (1971). Procedures for reacting to a change in distribution. *The Annals of Mathematical Statistics*, **42** 1897–1908.
- MADRID PADILLA, O. H., ATHEY, A., REINHART, A. and SCOTT, J. G. (2019). Sequential non-parametric tests for a change in distribution: an application to detecting radiological anomalies. *Journal of the American Statistical Association*, **114** 514–528.
- MOUSTAKIDES, G. V. (1986). Optimal stopping times for detecting changes in distributions. *The Annals of Statistics*, **14** 1379–1387.
- PAGE, E. S. (1954). Continuous inspection schemes. *Biometrika*, **41** 100–115.
- R CORE TEAM (2020). *R: A Language and Environment for Statistical Computing*. R Foundation for Statistical Computing, Vienna, Austria. URL <https://www.R-project.org/>.
- RITOV, Y. (1990). Decision theoretic optimality of the cusum procedure. *The Annals of Statistics* 1464–1469.
- WANG, D., YU, Y. and RINALDO, A. (2018). Optimal change point detection and localization in sparse dynamic networks. *arXiv preprint arXiv:1809.09602*.
- XU, J. (2017). Rates of convergence of spectral methods for graphon estimation. *arXiv preprint*.
- XU, J. (2018). Rates of convergence of spectral methods for graphon estimation. In *International Conference on Machine Learning*. 5433–5442.
- YOUNG, S. J. and SCHEINERMAN, E. R. (2007). Random dot product graph models for social networks. In *International Workshop on Algorithms and Models for the Web-Graph*. 138–149.
- YU, Y., PADILLA, O. H. M., WANG, D. and RINALDO, A. (2020). A note on online change point detection. *arXiv preprint arXiv:2006.03283*.
- ZHANG, Y., WAINWRIGHT, M. J. and DUCHI, J. C. (2012). Communication-efficient algorithms for statistical optimization. In *Advances in Neural Information Processing Systems*. 1502–1510.